Published Ahead of Print on January 5, 2017, as doi:10.3324/haematol.2016.153841.

IL21R expressing CD14+CD16+ monocytes expand in multiple myeloma patients leading to increased osteoclasts

by Marina Bolzoni, Domenica Ronchetti, Paola Storti, Gaetano Donofrio, Valentina Marchica, Federica Costa, Luca Agnelli, Denise Toscani, Rosanna Vescovini, Katia Todoerti, Sabrina Bonomini, Gabriella Sammarelli, Andrea Vecchi, Daniela Guasco, Fabrizio Accardi, Benedetta Dalla Palma, Barbara Gamberi, Carlo Ferrari, Antonino Neri, Franco Aversa, and Nicola Giuliani

Haematologica 2017 [Epub ahead of print]

Citation: Bolzoni M, Ronchetti D, Storti P, Donofrio G, Marchica V, Costa F, Agnelli L, Toscani D, Vescovini R, Todoerti K, Bonomini S, Sammarelli G, Vecchi A, Guasco D, Accardi F, Dalla Palma B, Gamberi B, Ferrari C, Neri A, Aversa F, and Giuliani N. IL21R expressing CD14+CD16+ monocytes expand in multiple myeloma patients leading to increased osteoclasts.
Haematologica. 2017; 102:xxx
doi:10.3324/haematol.2016.153841

IL21R expressing CD14^{+}CD16^{+} monocytes expand in multiple myeloma patients leading to increased osteoclasts.

Marina Bolzoni,[1] Domenica Ronchetti,[2,3] Paola Storti,[1,4] Gaetano Donofrio,[5] Valentina Marchica,[1,4] Federica Costa,[1] Luca Agnelli, [2,3] Denise Toscani,[1] Rosanna Vescovini,[1] Katia Todoerti,[6] Sabrina Bonomini,[7] Gabriella Sammarelli,[1,7] Andrea Vecchi,[8] Daniela Guasco,[1] Fabrizio Accardi,[1,7] Benedetta Dalla Palma,[1,7] Barbara Gamberi,[9] Carlo Ferrari,[8] Antonino Neri,[2,3] Franco Aversa,[1,4,7] and Nicola Giuliani.[1,4,7]

[1]Myeloma Unit, Dept. of Clinical and Experimental Medicine, University of Parma, Parma, Italy;
[2]Dept. of Oncology and Hemato-Oncology, University of Milan, Milan, Italy;
[3]Hematology Unit, "Fondazione IRCCS Ca' Granda", "Ospedale Maggiore Policlinico", Milan, Italy;
[4] CoreLab, "Azienda Ospedaliero-Universitaria di Parma", Parma, Italy;
[5]Dept. of Medical-Veterinary Science, University of Parma, Parma, Italy;
[6]Laboratory of Pre-clinical and Translational Research, IRCCS-CROB, Referral Cancer Center of Basilicata, Rionero in Vulture, Italy
[7]Hematology and BMT Center, "Azienda Ospedaliero-Universitaria", Parma, Italy;
[8]Infectious Disease Unit, "Azienda Ospedaliero-Universitaria", Parma, Italy;
[9]"Dip. Oncologico e Tecnologie Avanzate", "IRCCS Arcispedale Santa Maria Nuova", Reggio Emilia, Italy.

Running heads: Molecular features of monocytes in myeloma.

Contact information for correspondence:
Nicola Giuliani, MD, PhD
Dept. of Clinical and Experimental Medicine, University of Parma
Via Gramsci 14, 43126, Parma, Italy
Tel: +39-0521-033299; Fax: +39-0521-033264
Email: nicola.giuliani@unipr.it

Word count: 4000
Number of tables: 3
Number of figures: 6
Number of supplemental files: 1

Acknowledgements:
This work was supported in part by a grant from the Associazione Italiana per la Ricerca sul Cancro (AIRC) IG2014 n.15531 (NG), a fellowship Fondazione Italiana per la Ricerca sul Cancro id. 18152 (MB), a fellowship Fondazione Italiana per la Ricerca sul Cancro id. 16462 (DT), AIRC IG16722 (AN)

Abstract

Bone marrow monocytes are primarily committed to osteoclast formation. It is, however, unknown whether potential primary alterations are specifically present in bone marrow monocytes of multiple myeloma patients, smoldering myeloma or monoclonal gammopathy of uncertain significance. Herein, we analyzed the immunophenotypic and transcriptional profiles of bone marrow $CD14^+$ monocytes in a cohort of patients with different types of monoclonal gammopathies to identify alterations involved in myeloma-enhanced osteoclastogenesis. A higher number of bone marrow $CD14^+CD16^+$ cells was found in patients with active myeloma as compared to those with smoldering myeloma and monoclonal gammopathy of uncertain significance. Interestingly, sorted bone marrow $CD14^+CD16^+$ cells from myeloma patients were more pro-osteoclastogenic than $CD14^+CD16^-$ cells in cultures *ex vivo*. Moreover, transcriptional analysis demonstrated that bone marrow multiple myeloma (but neither monoclonal gammopathy of uncertain significance nor smoldering myeloma) $CD14^+$ cells significantly upregulated genes involved in osteoclast formation, including *IL21R*. *IL21R* mRNA over-expression by bone marrow $CD14^+$ cells was independent from the presence of IL-21. Consistently, IL-21 production by T cells as well as IL-21 bone marrow levels were not significantly different among monoclonal gammopathies. Thereafter, we showed that *IL21R* over-expression in $CD14^+$ cells increased osteoclast formation. Consistently, IL-21R signaling inhibition by Janex 1 suppressed osteoclast differentiation from bone marrow $CD14^+$ cells of myeloma patients. Our results indicated that multiple myeloma patients showed distinct bone marrow monocyte features compared to those with indolent monoclonal gammopathies, supporting the role of *IL21R* over-expression by bone marrow $CD14^+$ cells in enhanced osteoclast formation.

Keywords: Multiple myeloma, Monoclonal gammopathy of undetermined significance, Bone marrow microenvironment, Osteoclast, Monocyte

INTRODUCTION

Multiple myeloma (MM) is characterized by bone destruction, osteolytic lesions and consequently a higher fracture risk[1] due to an increase in bone marrow (BM) osteoclast (OC) formation and osteoblast suppression.[2-4] Conversely, patients with indolent gammopathies such as smoldering MM (SMM) and monoclonal gammopathy of uncertain significance (MGUS) are characterized by the absence of lytic lesions, although an increase in OC bone resorption may occur.[5-9]

Since the close relationship between plasma cells (PCs) and BM microenvironment plays a pivotal role in MM pathogenesis,[10] ongoing studies are focusing on the presence of potential molecular alterations in the microenvironment.[11-13] Transcriptional profile alterations have been reported in mesenchymal stromal cells (MSCs) and osteoblasts of MM patients correlated to osteolytic lesions and when compared to healthy donors but not MGUS patients.[13] BM monocytes play a pivotal role in bone disease,[2, 4, 14] angiogenesis[15] and immune system dysfunction,[16] which are hallmarks of active MM.

Enhanced bone resorption in MM patients occurs in the BM in close contact with PC infiltration.[5] Contact between MM cells and BM stromal cells stimulates the production of the Receptor Activator of Nuclear factor Kappa-B Ligand (RANKL), the main pro-osteoclastogenic cytokine involved in OC differentiation, through its receptor RANK on monocytes surface.[2, 17] Moreover, different factors produced by MM cells can stimulate osteoclastogenesis including Interleukin (IL)-6[18] and the Macrophage Inflammatory Protein (MIP)-1α.[19, 20] Recently, it has also been reported that IL-3 is increased in BM plasma from MM patients and that it induces Activin A production by BM monocytes which in turn stimulates osteoclastogenesis in a RANKL-independent mechanism.[21] This suggests that BM monocytes may be directly involved in enhanced osteoclastogenesis in MM.

Immunophenotypic analysis of peripheral monocytes demonstrates that $CD14^+CD16^+$ sub-population accounts for 5–10% of monocytes in healthy individuals but resulted significantly expanded in cancer[22] and inflammatory conditions.[23, 24] In psoriatic arthritis, $CD14^+CD16^+$ cells have been associated to bone erosion and identified as the main source of OC progenitors.[25] More recently, it has been reported that the proportion of $CD14^+CD16^+$ cells increased in MM patients with the tumor load[26, 27] and these cells are potential markers of OC progenitors.[27] However, the presence of alterations in the BM monocytes in MM patients is still unknown. Thus, the aim of this study was the characterization of the immunophenotypic and transcriptional profiles of the BM $CD14^+$ cells across a cohort of patients with different types of monoclonal gammopathies in order to identify genes that are potentially involved in enhanced osteoclastogenesis and possibly druggable as new therapeutic targets.

METHODS

Patients

A total cohort of 50 patients with newly diagnosed active MM 32 patients with smoldering MM (SMM), and 20 patients with monoclonal gammopathy of undetermined significance (MGUS) admitted to our hematological Institution from 2010 until 2016 were included in the analysis of monocytes features. All of the subjects involved in the study gave their written informed consent, according to the Declaration of Helsinki. The University of Parma's Institutional Review Board (Parma, Italy) approved all the study protocols. To define the presence of osteolytic lesions in MM patients we used the X-ray skeletal survey as first imaging procedure and alternatively a CT low dose scan or CT/PET scan evaluations, as recently updated by the International Myeloma Working Group.[28] The evaluation of the skeleton was performed in MM patients at the same period of the BM aspirates. The presence of at least one lytic lesion on X-ray or CT/PET scan was used to define osteolytic patients. The presence of equal or more than three lytic lesions was used to define high bone disease (HBD) patients. MM patients with low bone disease (LBD) were considered with minus of 3 lytic lesions or without bone lesions.[29]

Specifically, patient samples were not suitable for all the analysis performed. Table 1 reports the number of patients analyzed by the different techniques used in the study.

Primary cell isolation and characterization.

Immunophenotype. Details of the immunophenotype analysis performed were reported in on-line Supplemental data.

Isolation of primary $CD14^+$ cells and $CD14^+$ cell sorting from BM samples.

$CD14^+$ monocytes were isolated from BM and peripheral blood (PB) mononuclear cells (MNCs) by immunomagnetic method with anti-CD14 mAb conjugated with microbeads (Miltenyi Biotech; Bergisch-Gladbach, Germany).

With the same protocol, $CD138^+$, $CD3^+$, $CD4^+$ and $CD8^+$ cells were isolated from BM samples. The presence of potential contaminating cells in each fraction was evaluated by flow cytometry analysis, using the fluorescence-activated flow cytometer BD FACS Canto II with Diva software (Becton, Dickinson and Company (BD); Franklin Lakes, NJ). Purity of monocyte samples was >92% and an example of purity analysis is shown in Supplemental Figure 1. All the Abs (anti-human CD14-PerCP-Cy5.5, clone MφP9; anti-human CD138 PE, clone MI15; anti-human CD3 FITC, clone SK7; anti-human CD4 FITC, Clone L120; anti-human CD8 PE, Clone SK1) were obtained from BD.

Primary BM MSCs were obtained from the $CD14^-CD138^-$ fraction of BM MNCs. Cells were incubated until confluence for 2 weeks in alpha minimum essential medium (αMEM) supplemented with glutamine, at 15% fetal bovine serum (FBS) (all these reagents purchased from Invitrogen Life Technologies; Carlsbad, CA).

For $CD14^+$ cell sorting, purified BM $CD14^+$ cells were stained with PE-Cy7-conjugated anti-CD16 Ab and sorted according to the gating strategy shown in Supplemental Figure 2. The cells and gates were analyzed by FACSDivaTM 7 software (BD) and the cell sorting performed on the FACS Aria III instrument.

Fluorescence *in situ* hybridization (FISH), microarrays analysis and Real Time PCR.

These methodologies were detailed in Supplemental Methods section of on-line Supplemental data.

Cell culture conditions.

Monocyte treatment with cytokines.

Primary $CD14^+$ cells were cultured in the presence or absence of recombinant human (rh) IL-21 (30 pg/ml) (Biovision Inc.; Milpitas, CA) for 24 h and then collected for mRNA analysis.

The human monocytic cell line THP-1 was purchased from the American Type Culture Collection (Rockville, MD), recently authenticated and tested for mycoplasma contamination.

THP-1 cells were treated with rhIL-6 (20 ng/ml) (Thermo Scientific; Rockford, IL) and/or rh Tumor necrosis factor (TNF)-α (10 ng/ml) (OriGene; Rockville, MD) for 48 h and then collected for mRNA analysis.

Lentiviral infections.

The amplified *IL21R* complementary DNA sequence was cloned into the pLenti-GIII-CMV-GFP-2A-Puro lentiviral vector (Applied Biological Materials Inc.; Richmond, Canada). Recombinant lentivirus was produced by transient transfection of 293T cells.[30] Primary $CD14^+$ cells were transduced following published protocols.[31] Briefly, $8x10^6$ $CD14^+$ cells purified from PB buffy coats of healthy donors were placed in well plate in 2 ml of αMEM with 10% FBS and rhM-CSF (25ng/ml) (Peprotech; Rocky Hill, NJ) in the presence of either empty or IL21R vector. As a control, $CD14^+$ cells were also seeded in the same conditions without adding the lentiviral vector. After 18 h, 2 ml of fresh αMEM with 10% FBS and rhM-CSF (25 ng/ml) were added. After 3 days, cells were collected and seeded for osteoclastogenesis assays and for *IL21R* mRNA analysis.

Osteoclastogenesis assays.

After cell sorting, both $CD14^+CD16^-$ and $CD14^+CD16^+$ populations were seeded $2x10^5$ cells/well in 96well plates in αMEM with 10% FBS, rhM-CSF at 25 ng/ml and rhRANKL (Peprotech) at 60 ng/ml and then cultured for 28 days, replacing half medium every 2-3 days.

In another osteoclastogenesis assay setting, $2x10^5$ lentiviral transduced $CD14^+$ cells/well were seeded in 96well plates in αMEM medium with 10% FBS, rhM-CSF 10ng/ml and rhRANKL 50 ng/ml and the IL-21R signaling inhibitor Janex 1 (10 μM) (Cayman Chemical Company; Ann Arbor, MI) and then cultured for 28 days, replacing half medium every 2-3 days.

Finally, in the third osteoclastogenesis assay setting, MM BM MNCs or purified BM $CD14^+$ cells were used (n=18). $4x10^5$ MNCs or $2x10^5$ $CD14^+$ cells/well were seeded in 96well plates

in αMEM with 10% FBS, rhM-CSF 25 ng/ml and rhRANKL 20 or 60 ng/ml in presence or absence of rhIL-21 (30 pg/ml) and Janex 1 (10 μM), and then cultured for 28 days, replacing half medium every 2-3 days.

In all *in vitro* osteoclastogenesis assays, each condition was performed at least in triplicate. The OCs were identified and counted by light microscopy at the end of the culture period as multinucleated (>3 nuclei) cells positive for tartrate resistant acid phosphatase (TRAP) assay (Sigma Aldrich; Saint Louis, MO). OC areas were quantified using ImageJ software (U.S. National Institutes of Health, Bethesda, MD).

STAT3 activity assay.

The specific procedures were detailed in Supplemental Method section of on-line Supplemental data.

BM IL-21 levels in patients with monoclonal gammopathies.

The levels of IL-21 in BM plasma were measured by ELISA method as reported in on-line Supplemental data.

Statistical analysis.

Quantitative variables were compared by not-parametric Kruskal-Wallis and Mann-Whitney test, or parametric two-tail Student's t test. Results were considered significant at $p<0.05$. GraphPad Prism 5.0™ was used for all the statistical analyses.

RESULTS

MM patients show a higher number of BM $CD14^+CD16^+$ cells compared to MGUS.

The immunophenotype of BM $CD14^+$ cells was evaluated in BM aspirates of 28 active MM patients (median age 73 years, range 48-89; 46% female (F), 54% male (M); International Staging System (ISS): I=3 , II=8, III=17); 15 SMM (median age 57 years, range 38-82; 33% F, 67% M) and 9 MGUS (median age 57 years, range 37-78; 44% F, 54% M). 48% of active MM patients had evidence of osteolytic lesions. A representative example of flow cytometry analysis is reported in Figure 1A.

We found that the median % of $CD14^+CD16^+$ cells in BM samples significantly increased across the different types of monoclonal gammopathies from MGUS to active MM: MGUS: 1.9% (range: 0-3%), n=9; SMM: 3.5% (range: 1.0-7.5%), n=15; active MM: 5.25% (range: 0-20.0%), n=28; p=0.0071.

In particular a statistically significant difference was observed comparing MM and MGUS patients (p=0.0144) (Figure 1B).

There was no statistical difference in the median % of BM $CD14^+CD16^+$ population between osteolytic MM patients (n=13) *versus* not-osteolytic ones (n=15): 4% (range 0-20%) *versus* 7.8% (range 0-20%), respectively (Figure 1C). Similarly, comparing MM patients with HBD (n=9) *versus* those with LBD (n=19), we did not find a statistically significant difference in the median % of BM $CD14^+CD16^+$ population: 4.7% (range 0-20%) *versus* 5.5% (range 0-20%), respectively (Figure 1D).

In the same way, analyzing all myeloma patients (SMM and MM), there was no significance difference between the osteolytic patients compared to those without osteolytic lesions [osteolytic MM (n=13) *versus* not-osteolytic MM plus SMM (n=30): 4% (range: 0-20%) *versus* 4.3% (range: 0-20%)].

BM $CD14^+CD16^+$cells in MM patients are pro-osteoclastogenic in *ex vivo* cultures.

To investigate whether the increased number of $CD14^+CD16^+$ cells observed in the BM samples of MM patients could be associated with an enhanced pro-osteoclastogenic activity, we sorted the BM $CD14^+CD16^+$ monocyte population by FACS and then tested its *ex vivo* pro-osteoclastogenic differentiation properties in comparison with the $CD14^+CD16^-$ cell fraction. A representative example of flow cytometry analysis of monocyte sub-populations before and after cell sorting was reported in Supplemental Figure 2. A median value of $3.5x10^5$ of $CD14^+CD16^+$ was obtained after cell sorting from MM BM samples. Due to the limited numbers of cells, we were only able to perform osteoclastogenesis assays. Interestingly, we found that $CD14^+CD16^+$ cells generated more TRAP positive cells with a higher number of OCs showing 5 or more nuclei than $CD14^+CD16^-$ population (Figure 1 E).

A different transcriptional fingerprint characterizes BM $CD14^+$ cells in MM patients as compared to SMM and MGUS.

We performed gene expression profiles of purified primary BM monocytes. We checked the intensity value of specific *CD14* and *CD138* probe sets (Supplemental Table 1) and discarded 9 samples displaying high *CD138* expression from the analysis to further ensure to exclude the presence of malignant PCs in the analysis. Hence, BM monocyte samples included in the gene expression analysis were obtained from 23 MM, 15 SMM and 9 MGUS patients. The main characteristics of patients eligible for gene expression analysis were reported in Table 2. Unsupervised analysis significantly clustered together MM samples (p=0.0024, Fischer's exact test) whereas SMM and MGUS were scattered along the dendrogram. (Figure 2A). A multiclass analysis identified 99 differentially expressed genes in $CD14^+$ cells between the three classes of patients (Supplemental Figure 3A; Supplemental Table 2), whereas 78 genes (18 up- and 60 down-regulated) were differentially expressed in monocytes of MM patients

as compared to SMM (Supplemental Figure 3B; Supplemental Table 3). The comparison of MM with asymptomatic samples (SMM and MGUS) identified 254 genes differentially expressed in $CD14^+$ cells, specifically, 62 up-regulated and 192 down-regulated genes (Supplemental Figure 3C; Supplemental Table 4). Functional annotation analysis of genes differentially expressed in symptomatic patients was performed using standard procedure in Database for Annotation, Visualization and Integrated Discovery (DAVID) and Gene Set Enrichment Analysis (GSEA) tools (Table 3). Among the identified gene sets, it is worth mentioning those associated with the Cytokine-cytokine receptor interaction pathway, Jak-STAT signaling pathway, and the interferon alpha and gamma responses. Among the differentially expressed genes, chemokines and chemokine and cytokine receptors with pro-osteoclastogenic properties such as *CCR5*, *IL21R* and *CD40*, were specifically up-regulated in $CD14^+$ of MM patients. Importantly, monocytes in MM samples up-regulate *SLAMF7*, which is selectively expressed in plasma cells and natural killer cells in MM leading to antibody-dependent cellular cytotoxicity and direct natural killer cell activation.[32] Particularly, *IL21R* over-expression by BM $CD14^+$ in MM patients was demonstrated (q-value=0), either in the multiclass analysis or comparing MM *versus* SMM plus MGUS (Supplemental Table 2 and 4). Interestingly, *IL21R* gene expression in the complete database significantly correlated with the expression of *CCR5* (p=0.0197), *CD40* (p<0.0001), and *SLAMF7* (p=0.0002) genes (Figure 2B). Moreover a further analysis between osteolytic *versus* not-osteolytic active MM patients identified 12 genes (*SERPINB10; CDCA5; MYBL2; SELENBP1; TK1; GYPA; KIF18A; SPC25; HJURP; TAL1; SKA1*) down regulated in not-osteolytic MM patients. On the other hand, we did not find a significant different gene expression signature between high bone disease *versus* low bone disease active MM patients. Thereafter, in a subgroup of patients, we confirmed a significant up-regulation of *IL21R*, *CCR5*, *CD40*, and *SLAMF7* genes in $CD14^+$ cells from MM patients compared to SMM

and/or MGUS, by Real Time PCR (Figure 2C). Consistently with the GEP data, we did not find a significant different expression of *IL21R*, *CCR5*, *CD40*, and *SLAMF7* genes between osteolytic *versus* not-osteolytic active MM patients (Figure 2D).

BM CD14$^+$ cells over-express *IL21R* mRNA in MM patients irrespective of IL-21.

Based on the gene expression data and the previous evidences that IL-21 is a growth factor for MM cells[33, 34] and IL-21/IL21R axis promotes osteoclastogenesis and bone destruction in pathological conditions[35, 36] we further investigated the possible role of *IL21R* over-expression by CD14$^+$ cells in MM-induced osteoclastogenesis.

Firstly, by means of Real Time PCR, we confirmed that *IL21R* mRNA levels significantly increased in BM CD14$^+$ cells across different PC dyscrasias in a cohort of patients with MM, SMM and MGUS (p=0.036) (Figure 3A). We showed that BM CD14$^+$ cells expressed significantly higher levels of *IL21R* mRNA in MM patients as compared to MGUS (p=0.023, Figure 3A), and in MM compared to SMM plus MGUS patients (p=0.005, Figure 3B). The up-regulation of *IL21R* mRNA was also observed in MM CD14$^+$ cells obtained from PB (n=3, data not shown). The mean difference between *IL21R* expression (expressed as -ΔCt) by BM and PB monocytes purified from the same patient was 0.46±0.49 (p= 0.64). The expression of IL-21R was also investigated at protein level by flow cytometry: in line with the evidence that CD14$^+$CD16$^+$ population was increased in MM patients, we found that BM CD14$^+$ cells in MM patients expressed IL-21R/CD360 and that CD14$^+$CD16$^+$ population showed higher median fluorescence intensity (MFI) compared to CD14$^+$CD16$^-$ cells in each tested patient (mean $\Delta_{MFICD14+CD16+-MFICD14+CD16-}$ ±SD= 6.1±2.4) (Figure 3C).

Furthermore, we checked the levels of active STAT3 in BM CD14$^+$ cells, as it is well known that the signaling pathway down-stream of IL-21R leads to the activation of Jak3 and STAT3.[37, 38] We found that MM CD14$^+$ cells had significantly higher levels of active STAT3

compared to MGUS (p=0.0029) and asymptomatic ones (MGUS plus SMM) (p=0.0093, Figure 3D).

To investigate the possible mechanisms involved in *IL21R* mRNA over-expression, we treated purified BM $CD14^+$ cells obtained from MM or SMM or MGUS patients with the rhIL-21 concentration reached in the BM plasma of our cohort of patients. The addition of rhIL-21 (30 pg/ml) slightly increase *IL21R* mRNA in BM $CD14^+$ cells from MGUS and SMM patients but not from MM patients, without reaching the statistically significance difference (Figure 3E), suggesting a constitutive *IL21R* mRNA expression in MM patients irrespective of the presence of IL-21. On the other hand, using the well-establish[39] monocytic cell line THP-1, we found that the combined treatment with pro-inflammatory cytokines rhIL-6 (20 ng/ml) and rhTNF-α (10 ng/ml) significantly increased *IL21R* mRNA expression compared to untreated controls (p=0.005, Figure 3F).

BM IL21 expression and levels did not significantly differ across patients with monoclonal gammopathies.

Next, we evaluated *IL21* mRNA expression levels in our cohort of patients. BM MSCs, $CD14^+$ and primary MM cells did not express *IL21* gene, which was otherwise expressed by $CD3^+$ cells, in the $CD4^+$ fraction, checked by Real Time PCR (Supplementary Table 5). We failed to find a significant difference in *IL21* mRNA expression by $CD3^+$ cells among MM, SMM and MGUS patients, as reported in Figure 4A. Consistently, no significant difference was found in BM levels of IL-21 across the different monoclonal gammopathies, as detected by ELISA (Figure 4B). The median BM IL-21 level was of 32.4 pg/ml for MGUS, 24.4 pg/ml for SMM and 34.1 pg/ml for newly diagnosed MM patients.

***IL21R* over-expression by $CD14^+$ cells is involved in osteoclastogenesis.**

Since *IL21R* has been identified among the genes over-expressed by BM $CD14^+$ cells in MM patients, we therefore investigated its role in OC differentiation. We induced *IL21R* over-

expression in $CD14^+$ cells obtained from 3 different healthy donors. The over-expression of *IL21R* gene was evaluated by Real Time PCR in $CD14^+$ cell infected with IL-21R vector ($CD14^+$ IL21R vector) and compared to those infected with the empty vector ($CD14^+$ empty vector, Figure 5A). Subsequently, we performed *in vitro* osteoclastogenesis assays. The number of OCs in this set of experiments was low because the infection with lentiviral vectors highly affects primary monocyte viability (Figure 5B-C). Interestingly, *in vitro* osteoclastogenesis assays showed that the over-expression of *IL21R* increased the number and median area of OCs in the presence of RANKL and M-CSF compared to controls; consistently, the presence of Janex 1, a JAK3 inhibitor known to block IL-21R signaling, significantly reduced OC formation and size in $CD14^+$ IL21R vector cells (Figure 5B-C).

Blocking IL-21R signaling inhibits osteoclastogenesis.

To further confirm the role of *IL21R* over-expression in osteoclastogenesis, we performed *in vitro* osteoclastogenesis assays with or without rhIL-21 in the presence or absence of Janex 1. The presence of rhIL-21 did not affect the number and the area of TRAP positive OCs obtained from total MNCs or $CD14^+$ cells purified from MM BM aspirates (Figure 6A-B). Any significant difference was not found in the number and in the OC area between tumor and not-tumor samples treated with IL-21 (data not shown).

On the other hand, Janex 1 significantly suppressed osteoclastogenesis, either from total BM MNCs or from BM $CD14^+$ cells obtained from MM patients, both in the presence ($p<0.001$) and in absence ($p<0.001$) of the rhIL-21, as shown in Figure 6 A-B. Moreover, the presence of Janex 1 significantly reduced the median OC area both in the presence ($p=0.012$) and in absence ($p<0.001$) of the rhIL-21 compared to untreated controls (Figure 6A).

DISCUSSION

Monoclonal gammopathies are characterized by the activation of bone resorption with progressive increase in the number of OCs from MGUS to MM.[5] Several studies have evaluated the gene expression profiles of PCs obtained both from patients with newly diagnosed MM and MGUS and from healthy donors to identify genes potentially related to the progression of MM.[40, 41] However, while MGUS and MM can be distinguished from normal PCs, these two conditions cannot be easily differentiated from each other.[40, 41] The transcriptional data were used to stratify MM patients with lytic lesions, identifying *DKK1* as the main over-expressed gene when focal bone lesions occur.[42] Studies analyzing the BM microenvironment cells indicate that MSCs and osteoblasts in MM patients have different transcriptional profiles, in comparison with healthy donors and based on the occurrence of osteolytic lesions.[13] However, all the BM biological alterations from MGUS to SMM and, finally, to active MM are not yet clear.

As regards the immunophenotypic profile, we found that the median percentage of $CD14^+CD16^+$ cells in BM samples increased among the different types of monoclonal gammopathies, resulting significantly higher in MM *versus* MGUS. In our study, for the first time we sorted BM $CD14^+CD16^+$ cells and showed that they represent the osteoclastogenic fraction of $CD14^+$ cells in MM patients, supporting the notion that inflammatory monocytes are involved in MM-induced osteoclastogenesis. In addition, $CD14^+CD16^+$ cells might contribute to the high production of inflammatory cytokines, such as TNF-α,[23] that are increased in the BM of MM patients and involved in OC formation.[43, 44]

Consistent with the immunophenotypic profile, the transcriptome of $CD14^+$ obtained from MM patients showed the up-regulation, as compared to SMM and MGUS, of genes involved in immune response, chemotaxis and osteoclastogenesis. We focused on genes potentially involved in osteoclastogenesis. Among the up-regulated genes, we found *CCR5*, whose role

in bone destruction in MM has already been extensively investigated.[19, 20] *IL21R* mRNA was also over-expressed by BM $CD14^+$ cells in MM but not in SMM or MGUS.

The analysis between osteolytic *versus* not-osteolytic active MM patients identified only few 12 genes down regulated in not-osteolytic MM patients. Nevertheless, we did not find a significant different gene expression signature between high bone disease *versus* low bone disease active MM patients. The lack of major differences in the immunophenotypic and transcriptional profiles of monocytes between osteolytic and not osteolytic are not surprising because the main pathophysiological difference between osteolytic and non osteolytic MM patients is the suppression of osteoblast formation rather than the increases osteoclast formation and activity. Our data are supported by previous studies reporting that all MM patients have a significant increase of bone resorption rate with an unbalanced bone remodeling.[5, 9] In addition, MGUS patients have a significant increase of bone resorption rate.[5, 7] Consistently in this study we lack to find a large number of differentially expressed genes by monocytes across patients with the different monoclonal gammopathies.

In this study, we demonstrated the potential involvement of IL-21/IL-21R axis in increased osteoclastogenesis that occurs in MM patients. The ligand of IL-21R, the cytokine IL-21, is a growth factor for MM cells[33, 34] and it is mainly produced by T cells.[37, 45] The binding of IL-21 to its receptor leads to the activation of the Jak–STAT pathway, in particular Jak1, Jak3, STAT1, and STAT3.[37, 46, 47] Interestingly, a previous study showed that IL-21 up-regulation in the synovium and the serum of rheumatoid arthritis patients is involved in osteoclastogenesis and bone destruction.[35] Nevertheless, its role in MM-induced OC formation is largely unknown. In this study we found a significant *IL21R* mRNA over-expression by $CD14^+$ cells correlated with the other osteoclastogenic genes identified such as *CCR5*, but also with *CD40* and *SLAMF7*. Interestingly, in line with the immunophenotypic profile of BM $CD14^+$ in MM patients, *IL21R* was expressed at high intensity in the

$CD14^+CD16^+$ fraction. The up-regulation of *IL21R* in MM patients was associated with an increase of STAT3 signaling and independent from the presence of IL-21. On the other hand, as the combination of the pro-inflammatory cytokines IL-6 and TNF-α increase *IL21R* mRNA expression in monocytes, we might suppose that these cytokines are involved in *IL21R* over-expression by BM $CD14^+$ cells. The pathophysiological role of *IL21R* over-expression by $CD14^+$ cells in enhanced osteoclastogenesis occurring in MM patients was further demonstrated by a lentiviral approach. These data also supported the role of IL-21R signaling as a potential therapeutic target. Accordingly, it is worth remembering that the clinically approved JAK3 inhibitor Tofacitinib suppresses OC-mediated structural damage to arthritic joints and decreases RANKL production.[48] This study is not designed to evaluate the role of IL-21R overexpression as a potential biomarker of MM progression, however our data suggest that IL-21R expression level could be a potential biomarker of myeloma progression. Clearly, only an appropriate prospective study evaluating the IL-21R expression could address to this point.

In conclusion, the study supports the notion that a pro-inflammatory profile of BM $CD14^+$ cells is involved in osteoclastogenesis in MM patients, in line with a considerable amount of evidences from literature.[19, 49, 50] For the first time, we highlighted *IL21R* over-expression in BM monocytes from MM patients and demonstrated its role in increased osteoclastogenesis, suggesting that IL-21R signaling could be a potential new therapeutic target for MM bone disease.

REFERENCES

1. Melton LJ, 3rd, Kyle RA, Achenbach SJ, Oberg AL, Rajkumar SV. Fracture risk with multiple myeloma: a population-based study. J Bone Miner Res. 2005;20(3):487-493.
2. Giuliani N, Colla S, Rizzoli V. New insight in the mechanism of osteoclast activation and formation in multiple myeloma: focus on the receptor activator of NF-kappaB ligand (RANKL). Exp Hematol. 2004;32(8):685-691.
3. Giuliani N, Rizzoli V, Roodman GD. Multiple myeloma bone disease: Pathophysiology of osteoblast inhibition. Blood. 2006;108(13):3992-3996.
4. Roodman GD. Pathogenesis of myeloma bone disease. Leukemia. 2009;23(3):435-441.
5. Bataille R, Chappard D, Basle MF. Quantifiable excess of bone resorption in monoclonal gammopathy is an early symptom of malignancy: a prospective study of 87 bone biopsies. Blood. 1996;87(11):4762-4769.
6. Kyle RA, Durie BG, Rajkumar SV, et al. Monoclonal gammopathy of undetermined significance (MGUS) and smoldering (asymptomatic) multiple myeloma: IMWG consensus perspectives risk factors for progression and guidelines for monitoring and management. Leukemia. 2010;24(6):1121-1127.
7. Ng AC, Khosla S, Charatcharoenwitthaya N, et al. Bone microstructural changes revealed by high-resolution peripheral quantitative computed tomography imaging and elevated DKK1 and MIP-1alpha levels in patients with MGUS. Blood. 2011;118(25):6529-6534.
8. Agarwal A, Ghobrial IM. Monoclonal gammopathy of undetermined significance and smoldering multiple myeloma: a review of the current understanding of epidemiology, biology, risk stratification, and management of myeloma precursor disease. Clin Cancer Res. 2013;19(5):985-994.
9. Bataille R, Chappard D, Marcelli C, et al. Mechanisms of bone destruction in multiple myeloma: the importance of an unbalanced process in determining the severity of lytic bone disease. J Clin Oncol. 1989;7(12):1909-1914.
10. Roodman GD. Role of the bone marrow microenvironment in multiple myeloma. J Bone Miner Res. 2002;17(11):1921-1925.
11. Corre J, Mahtouk K, Attal M, et al. Bone marrow mesenchymal stem cells are abnormal in multiple myeloma. Leukemia. 2007;21(5):1079-1088.
12. Garayoa M, Garcia JL, Santamaria C, et al. Mesenchymal stem cells from multiple myeloma patients display distinct genomic profile as compared with those from normal donors. Leukemia. 2009;23(8):1515-1527.
13. Todoerti K, Lisignoli G, Storti P, et al. Distinct transcriptional profiles characterize bone microenvironment mesenchymal cells rather than osteoblasts in relationship with multiple myeloma bone disease. Exp Hematol. 2010;38(2):141-153.
14. Yaccoby S, Wezeman MJ, Henderson A, et al. Cancer and the microenvironment: myeloma-osteoclast interactions as a model. Cancer Res. 2004;64(6):2016-2023.
15. Ribatti D, Vacca A. The role of monocytes-macrophages in vasculogenesis in multiple myeloma. Leukemia. 2009;23(9):1535-1536.
16. Kawano Y, Moschetta M, Manier S, et al. Targeting the bone marrow microenvironment in multiple myeloma. Immunol Rev. 2015;263(1):160-172.
17. Giuliani N, Bataille R, Mancini C, Lazzaretti M, Barille S. Myeloma cells induce imbalance in the osteoprotegerin/osteoprotegerin ligand system in the human bone marrow environment. Blood. 2001;98(13):3527-3533.
18. Bataille R, Chappard D, Klein B. The critical role of interleukin-6, interleukin-1B and macrophage colony-stimulating factor in the pathogenesis of bone lesions in multiple myeloma. Int J Clin Lab Res. 1992;21(4):283-287.
19. Choi SJ, Cruz JC, Craig F, et al. Macrophage inflammatory protein 1-alpha is a potential osteoclast stimulatory factor in multiple myeloma. Blood. 2000;96(2):671-675.

20. Han JH, Choi SJ, Kurihara N, Koide M, Oba Y, Roodman GD. Macrophage inflammatory protein-1alpha is an osteoclastogenic factor in myeloma that is independent of receptor activator of nuclear factor kappaB ligand. Blood. 2001;97(11):3349-3353.
21. Silbermann R, Bolzoni M, Storti P, et al. Bone marrow monocyte-/macrophage-derived activin A mediates the osteoclastogenic effect of IL-3 in multiple myeloma. Leukemia. 2014;28(4):951-954.
22. Lee HW, Choi HJ, Ha SJ, Lee KT, Kwon YG. Recruitment of monocytes/macrophages in different tumor microenvironments. Biochim Biophys Acta. 2013;1835(2):170-179.
23. Belge KU, Dayyani F, Horelt A, et al. The proinflammatory CD14+CD16+DR++ monocytes are a major source of TNF. J Immunol. 2002;168(7):3536-3542.
24. Ziegler-Heitbrock L. The CD14+ CD16+ blood monocytes: their role in infection and inflammation. J Leukoc Biol. 2007;81(3):584-592.
25. Chiu YG, Shao T, Feng C, et al. CD16 (FcRgammaIII) as a potential marker of osteoclast precursors in psoriatic arthritis. Arthritis Res Ther. 2010;12(1):R14.
26. Sponaas AM, Moen SH, Liabakk NB, et al. The proportion of CD16(+)CD14(dim) monocytes increases with tumor cell load in bone marrow of patients with multiple myeloma. Immun Inflamm Dis. 2015;3(2):94-102.
27. Petitprez V, Royer B, Desoutter J, et al. CD14+ CD16+ monocytes rather than CD14+ CD51/61+ monocytes are a potential cytological marker of circulating osteoclast precursors in multiple myeloma. A preliminary study. Int L Lab Hematol. 2015;37(1):29-35.
28. Rajkumar SV, Dimopoulos MA, Palumbo A, et al. International Myeloma Working Group updated criteria for the diagnosis of multiple myeloma. Lancet Oncol. 2014;15(12):e538-548.
29. Palma BD, Guasco D, Pedrazzoni M, et al. Osteolytic lesions, cytogenetic features and bone marrow levels of cytokines and chemokines in multiple myeloma patients: Role of chemokine (C-C motif) ligand 20. Leukemia. 2016;30(2):409-416.
30. Storti P, Donofrio G, Colla S, et al. HOXB7 expression by myeloma cells regulates their pro-angiogenic properties in multiple myeloma patients. Leukemia. 2011;25(3):527-537.
31. Ramnaraine ML, Mathews WE, Clohisy DR. Lentivirus transduction of human osteoclast precursor cells and differentiation into functional osteoclasts. Bone. 2012;50(1):97-103.
32. Markham A. Elotuzumab: First Global Approval. Drugs. 2016;76(3):397-403.
33. Brenne AT, Ro TB, Waage A, Sundan A, Borset M, Hjorth-Hansen H. Interleukin-21 is a growth and survival factor for human myeloma cells. Blood. 2002;99(10):3756-3762.
34. Menoret E, Maiga S, Descamps G, et al. IL-21 stimulates human myeloma cell growth through an autocrine IGF-1 loop. J Immunol. 2008;181(10):6837-6842.
35. Kwok SK, Cho ML, Park MK, et al. Interleukin-21 promotes osteoclastogenesis in humans with rheumatoid arthritis and in mice with collagen-induced arthritis. Arthritis Rheum. 2012;64(3):740-751.
36. Kim KW, Kim HR, Kim BM, Cho ML, Lee SH. Th17 Cytokines Regulate Osteoclastogenesis in Rheumatoid Arthritis. Am J Pathol. 2015;185(11):3011-3024.
37. Mehta DS, Wurster AL, Grusby MJ. Biology of IL-21 and the IL-21 receptor. Immunol Rev. 2004;202:84-95.
38. Ma J, Ma D, Ji C. The role of IL-21 in hematological malignancies. Cytokine. 2011;56(2):133-139.
39. Millet P, Vachharajani V, McPhail L, Yoza B, McCall CE. GAPDH Binding to TNF-alpha mRNA Contributes to Posttranscriptional Repression in Monocytes: A Novel Mechanism of Communication between Inflammation and Metabolism. J Immunol. 2016;196(6):2541-2551.
40. Zhan F, Hardin J, Kordsmeier B, et al. Global gene expression profiling of multiple myeloma, monoclonal gammopathy of undetermined significance, and normal bone marrow plasma cells. Blood. 2002;99(5):1745-1757.
41. Davies FE, Dring AM, Li C, et al. Insights into the multistep transformation of MGUS to myeloma using microarray expression analysis. Blood. 2003;102(13):4504-4511.

42. Tian E, Zhan F, Walker R, et al. The role of the Wnt-signaling antagonist DKK1 in the development of osteolytic lesions in multiple myeloma. N Engl J Med. 2003;349(26):2483-2494.
43. Lichtenstein A, Berenson J, Norman D, Chang MP, Carlile A. Production of cytokines by bone marrow cells obtained from patients with multiple myeloma. Blood. 1989;74(4):1266-1273.
44. Portier M, Zhang XG, Ursule E, et al. Cytokine gene expression in human multiple myeloma. Br J Haematol. 1993;85(3):514-520.
45. Caprioli F, Sarra M, Caruso R, et al. Autocrine regulation of IL-21 production in human T lymphocytes. J Immunol. 2008;180(3):1800-1807.
46. Asao H, Okuyama C, Kumaki S, et al. Cutting edge: the common gamma-chain is an indispensable subunit of the IL-21 receptor complex. J Immunol. 2001;167(1):1-5.
47. Zeng R, Spolski R, Casas E, Zhu W, Levy DE, Leonard WJ. The molecular basis of IL-21-mediated proliferation. Blood. 2007;109(10):4135-4142.
48. LaBranche TP, Jesson MI, Radi ZA, et al. JAK inhibition with tofacitinib suppresses arthritic joint structural damage through decreased RANKL production. Arthritis Rheum. 2012;64(11):3531-3542.
49. Giuliani N, Lisignoli G, Colla S, et al. CC-chemokine ligand 20/macrophage inflammatory protein-3alpha and CC-chemokine receptor 6 are overexpressed in myeloma microenvironment related to osteolytic bone lesions. Cancer Res. 2008;68(16):6840-6850.
50. Tucci M, Stucci S, Savonarola A, et al. Immature dendritic cells in multiple myeloma are prone to osteoclast-like differentiation through interleukin-17A stimulation. Br J Haematol. 2013;161(6):821-831.

TABLES

Table 1: Number of patients analyzed for the monocytes features by the different techniques.

	Immunophenotype	GEP	Real Time PCR
MGUS	9	9	6
SMM	15	15	11
MM	28	32*	13

Abbreviations: GEP= gene expression profile

*= 9 out of 32 samples, displaying high CD138 expression, were excluded from the statistical analysis.

Table 2: Main clinical characteristics of the cohort of patients eligible for gene expression analysis.

							MM cell genetic alterations					
Patient	**sex**	**age**	**ISS**	**osteolysis**	**HBD**	**type**	**del(13q)**	**H**	**del(17p)**	**t(11;14)**	**t(4;14)**	**t(14;16)**
MGUS1	F	43				l						
MGUS2	F	52				l						
MGUS3	M	42										
MGUS4	M	78				k						
MGUS5	F	54				l						
MGUS6	M	77				k	-		-	-	-	-
MGUS7	M	43				k						
MGUS8	M	91				l						
MGUS9	F	50										
SMM1	F	67				l						
SMM2	F	72				l	-	+	-	-	+	-
SMM3	F	58				l						
SMM4	M	58				k						
SMM5	F	64				k						
SMM6	F	61				l						
SMM7	F	64				k	-	+	-	-	-	-
SMM8	M	56				k						
SMM9	M	70				k	-	-	-			
SMM10	F	67					-		-			
SMM11	F	76				k						
SMM12	M	83				k	+	-	-	+	-	-
SMM13	M	47				k						
SMM14	M	41				k						
SMM15	M	65				k	+	-	-	-	+	-
MM1	M	83	III	+	-	l						
MM2	M	75	III			k						
MM3	F	59	II	+	-	k	+		-	-	-	+
MM4	F	80	II	-	-	l	+		+	-	-	-
MM5	M	76	II	-	-	l	+		-	+	-	-
MM6	F	79	II	-	-	l	+	-	-	-	-	
MM7	M	69	I	+	+	k						
MM8	M	79	II	+	+	l						
MM9	M	57	I	+	-	l	+	-	+			
MM10	M	81	II	+	+	k	-	+	-	-	-	-
MM11	M	60	II			k						
MM12	F	78	II			l	-		-	-	-	-
MM13	M	73	III	+	+	k						

MM14	M	74	II	+	+	l	-					
MM15	F	73	II	-	-	l	-		-	+	-	-
MM16	M	70	I	-	-	k	-	-	-			
MM17	F	84	III	-	-	k	+	-	-	-	-	-
MM18	F	86	III			l						
MM19	M	73	II	+	-	l	-	-	-	-	-	-
MM20	M	56	III	-	-	k						
MM21	F	50	II	+	+	k	+	-	-	+	-	-
MM22	F	75	I	+	+	k			-			
MM23	F	77	III	-	-	k	-	-		-	-	-

Abbreviations: MGUS, Monoclonal Gammopathy of Undetermined Significance; SMM, Smoldering Multiple Myeloma; MM, Multiple Myeloma; F, female; M, male; ISS, International Staging System; HBD, High Bone Disease; H, Hyperdiploid.

Table 3: Functional annotations* of the representative genes distinguishing BM monocytes arisen from supervised analysis of MM *versus* (MGUS plus SMM) patients.

Database for **A**nnotation, **V**isualization and **I**ntegrated **D**iscovery (**DAVID**)		
Pathway Database	***Term***	***Genes*[§]**
KEGG	Cytokine-cytokine receptor interaction	*CCR5, IL21R, CSF3R, CD40*
	Jak-STAT signaling pathway	*IL21R, CSF3R,*
	Chemokine signaling pathway	*GNGT2, CCR5*
REACTOME	Metabolism of carbohydrates	*GOT2, GPI, PGM1, PGD, GYS1,*

Gene Set Enrichment Analysis (GSEA)	
Functional group category	***Genes*[§]**
INTERFERON ALPHA RESPONSE	EPSTI1, IFI27, IFITM1, ISG20, LAP3
INTERFERON GAMMA RESPONSE	CD40, EPSTI1, IFI27, ISG20, LAP3, PIM1, SLAMF7, STAT4, VAMP5

*DAVID Functional Annotation Tool v6.8 (https://david.ncifcrf.gov) and GSEA tool (http://software.broadinstitute.org/gsea) were used to classify genes into functional categories.

[§] Genes down-regulated in MM monocytes are underlined.

FIGURE LEGENDS

Figure 1: Immunophenotype of BM monocytes in patients with monoclonal gammopathies and their pro-osteoclastogenic *ex vivo* properties.

(A) CD14 and CD16 expression by BM monocytes in patients with monoclonal gammopathies: example of plots of flow cytometry data. **(B)** Box plot represents the median percentage values of $CD14^+CD16^+$ cells evaluated in BM samples obtained from patients with MGUS, SMM and MM (*p* calculated by Mann-Whitney test). Box plot represents the median percentage values of $CD14^+CD16^+$ cells evaluated in BM samples obtained from patients with (w) or without (w/o) osteolysis **(C)** and from patients with high bone disease (HBD) or low bone disease (LBD) **(D).**

$CD14^+$ cells were purified from BM samples of patients with monoclonal gammopathies by an immunomagnetic method and then sorted in the two sub-populations $CD14^+CD16^-$ and $CD14^+CD16^+$ by a Flow cell sorter as described in Materials and methods section. $CD14^+CD16^-$ or $CD14^+CD16^+$ cells (200.000 cells/well) were seeded in 96well plates in αMEM medium at 10% FBS with rhM-CSF 25ng/ml and rhRANKL 60ng/ml. After 28 days of culture, OCs were identified as multinucleated TRAP positive cells and counted by light microscopy. **(E)** Bar graph represents the median number of OCs/well of each condition, divided into OCs with ≥5 nuclei or <5 nuclei (*p* calculated by Mann-Whitney test, $CD14^+CD16^-$ *versus* $CD14^+CD16^+$ cells). On the right there is a representative image of the osteoclastogenesis assay stained by TRAP from BM sorted $CD14^+CD16^-$ and $CD14^+CD16^+$ cells (Original magnification 4x)**.**

Figure 2: Transcriptional fingerprints evaluated by gene expression profiling of purified BM $CD14^+$ cells from patients with different monoclonal gammopathies.

(A) Heatmap of the trancriptional profiles resulting from the unsupervised analysis of all the MM, SMM and MGUS monocyte samples. **(B)** Scatterplots visualize the correlation between *IL21R* expression and that of, *CD40*, *SLAMF7* and *CCR5* by BM monocytes arisen from gene expression analysis The lines represent the linear regression between each couple of genes**.** **(C)** Quantitative Real Time PCR of *IL21R*, *CCR5*, *CD40* and *SLAMF7* genes performed on BM monocytes samples purified from patients with monoclonal gammopathies. Values represent the median of the -ΔCt values of the reactions (*: fold change >1.5). (**D**) Quantitative Real Time PCR of *IL21R*, *CCR5*, *CD40* and *SLAMF7* genes performed on BM monocytes samples purified from MM patients with (w) or without (w/o) osteolysis. Values represent the mean of the -ΔCt values of the reactions.

Figure 3: IL-21R over-expression by BM CD14$^+$ cells in MM compared to SMM and MGUS patients.

(A) *IL21R* mRNA expression was evaluated by Real Time PCR in purified BM CD14$^+$ obtained from patients with monoclonal gammopathies. Box plot shows the median –ΔCt levels (*p* calculated by Mann-Whitney test). (**B**) *IL21R* mRNA expression was evaluated by Real Time PCR in purified BM CD14$^+$ obtained from MM patients *versus* SMM+MGUS patients. Box plot shows the median –ΔCt levels (*p* calculated by Mann-Whitney test). **(C)** CD360/IL-21R expression was evaluated by flow cytometry in BM CD14$^+$CD16$^-$ and CD14$^+$CD16$^+$ cells as shown for a representative MM patient. Flow cytometry analysis of CD360 expression by CD14$^+$CD16$^-$ cells **(*i*)** and CD14$^+$CD16$^+$ cells **(*ii*)** stained with anti-CD360 or control IgG1. **(*iii*)** Comparison between CD360 expression by CD14$^+$CD16$^-$ and CD14$^+$CD16$^+$ monocyte populations (MFI: median fluorescence intensity). **(D)** Active STAT3 levels were determined by the STAT family assay kit in nuclear extracts of purified BM CD14$^+$ cells obtained from MGUS (n=3), SMM (n=3) and MM (n=3) patients. Bar chart

represents the mean±SD level of active STAT3 checked as optical density (OD) at 450 nm with a reference wavelength of 620 nm, after subtracting the blank. **(E)** BM $CD14^+$ cells purified from patients with MM, SMM or MGUS were treated with or without rhIL-21 (30pg/ml) for 24 h. *IL21R* mRNA level was evaluated by Real Time PCR. Bar chart represents the median –ΔCt of *IL21R* mRNA of three replicates (Con: untreated control). **(F)** The monocytic cell line THP-1 was treated for 48 h with or without rhIL-6 (20ng/ml) or TNF-α (10ng/ml) or both cytokines. *IL21R* mRNA levels were evaluated by Real Time PCR in 3 independent experiments (*p* calculated by t test). Bar chart represents the mean±SD fold change of mRNA *IL21R* (Con: untreated control).

Figure 4: *IL21* mRNA expression by BM microenvironment and IL-21 BM levels in patients with MM, SMM and MGUS.

(A) *IL21* mRNA expression by purified $CD3^+$ cells from MM (n=5), SMM (n=7) or MGUS (n=7) patients evaluated by Real Time PCR. Bar chart shows the mean±SD –ΔCt of *IL21* mRNA. **(B)** BM IL-21 levels were evaluated by ELISA assay in a cohort of 76 newly diagnosed MM, 42 SMM and 41 MGUS patients. Scatter dot plot represents BM IL-21 levels in the cohort of patients with the lines representing median levels.

Figure 5: *IL21R* over-expression by a lentiviral vector in monocytes increases the OC differentiation.

(A) *IL21R* over-expression was performed in PB $CD14^+$ cells obtained from 3 different healthy donors transduced with a specific lentiviral vector for *IL21R* ($CD14^+$ IL21R vector) as compared to those infected with the empty control vector ($CD14^+$ empty vector) or not transduced ($CD14^+$). *IL21R* mRNA levels were checked by Real Time PCR. Bar graph represents the median –ΔCt levels of 3 independent experiments. $CD14^+$ transduced cells

with *IL21R* or empty lentiviral vectors (200.000 cells/well) were seeded in 96 well plates in αMEM medium at 10% FBS with rhM-CSF 10 ng/ml and rhRANKL 50 ng/ml in the presence or absence of the IL-21R signaling inhibitor Janex 1 (10 μM) or vehicle (DMSO). After 28 days of culture, OCs were identified as multinucleated (>3 nuclei) TRAP positive cells and counted by light microscopy. **(B)** Bar graph shows the mean±SD OC number for each well (*p* calculated by t test) in 3 independent experiments with $CD14^+$ from 3 different healthy donors (left panel). Box plot represents the OC area (*p* calculated by Mann-Whitney test) in a representative experiment performed at least in triplicate (right panel). **(C)** Images of the osteoclastogenesis assay stained by TRAP of $CD14^+$ IL21R vector and $CD14^+$ cells empty vector performed in the presence or absence of Janex 1 of one representative experiment (Original magnification 4x).

Figure 6: IL-21R signaling inhibition blocks IL-21R driven osteoclastogenesis.

BM MNCs, obtained from MM patients, were seeded at the concentration of $4x10^5$ cells/well in 96 well plates in αMEM medium at 10% FBS with rhM-CSF 25 ng/ml and rhRANKL 20 ng/ml in presence or absence of rIL-21 (30 pg/ml) and the IL-21R signaling inhibitor Janex 1 (10 μM) or vehicle (DMSO) for 28 days, replacing the medium every 3 days. At the end of culture period OCs were identified as multinucleated (>3 nuclei) TRAP positive cells and counted by light microscopy (Con: untreated control). **(A)** Bar graph represents the mean±SD OC number for each well (*p* calculated by t test) (upper panel). Box plot shows the OC area (p calculated by Mann-Whitney test) in one representative experiment performed at least in triplicate (lower panel). **(B)** Representative images of OCs stained with TRAP after 28 days of culture (Original magnification 4x).

Figure 1

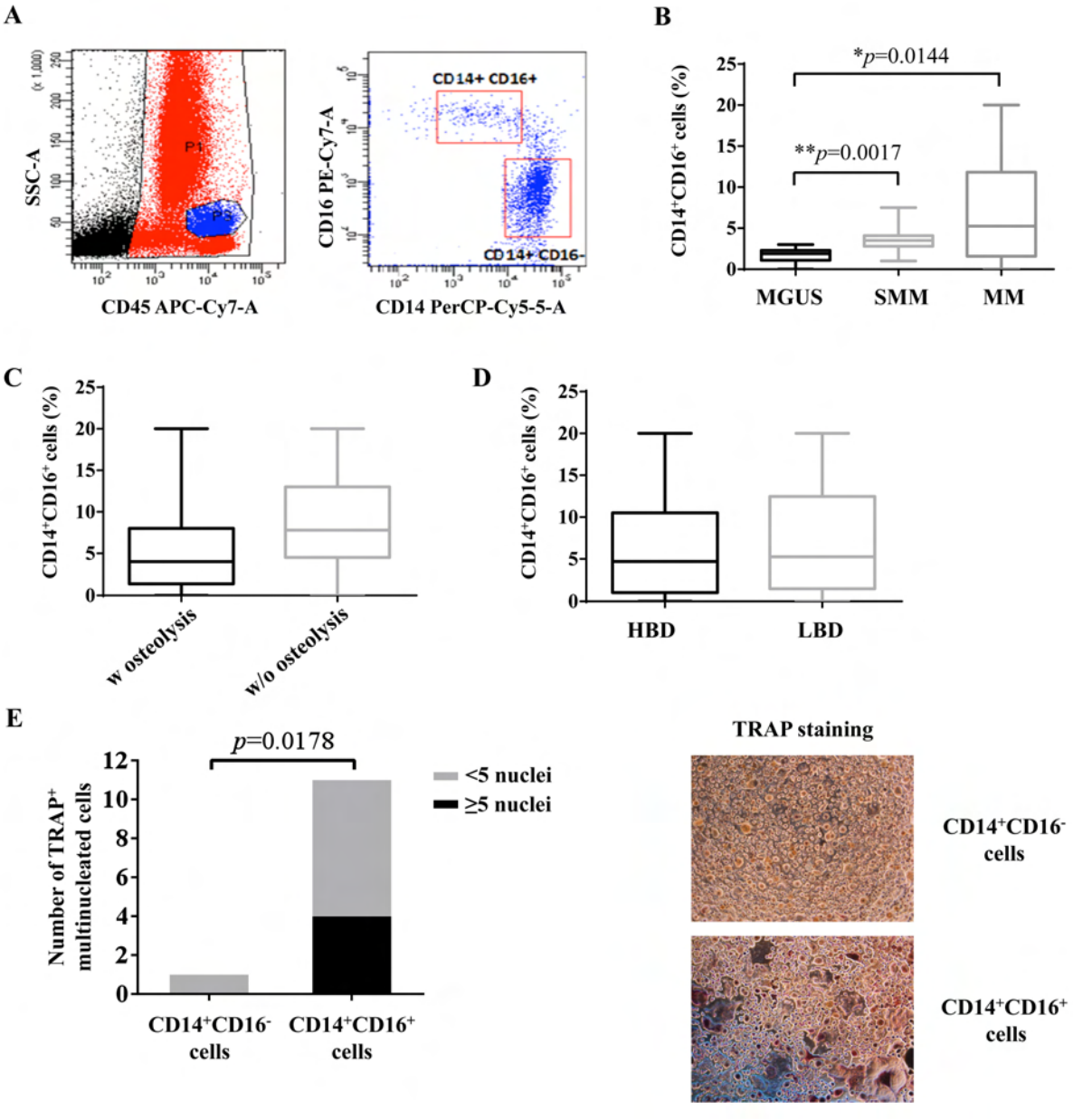
A
SSC-A
CD45 APC-Cy7-A
P1
P2
CD16 PE-Cy7-A
CD14 PerCP-Cy5-5-A
CD14+ CD16+
CD14+ CD16-
B
CD14+CD16+ cells (%)
*p=0.0144
**p=0.0017
MGUS
SMM
MM
C
CD14+CD16+ cells (%)
w osteolysis
w/o osteolysis
D
CD14+CD16+ cells (%)
HBD
LBD
E
p=0.0178
Number of TRAP+ multinucleated cells
<5 nuclei
≥5 nuclei
CD14+CD16- cells
CD14+CD16+ cells
TRAP staining
CD14+CD16- cells
CD14+CD16+ cells

Figure 2

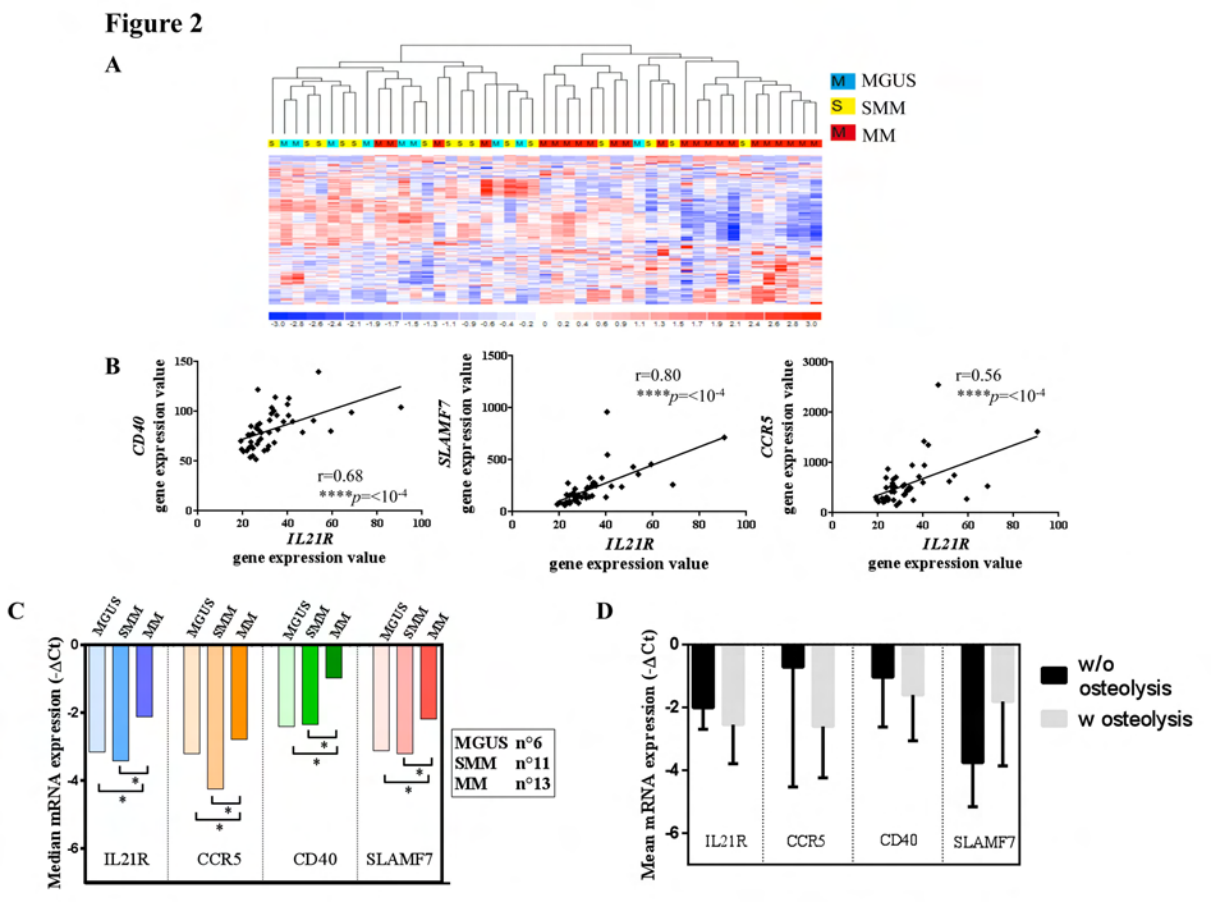
A
M MGUS
S SMM
M MM
B
CD40
gene expression value
r=0.68
****p=<10-4
IL21R
gene expression value
SLAMF7
gene expression value
r=0.80
****p=<10-4
IL21R
gene expression value
CCR5
gene expression value
r=0.56
****p=<10-4
IL21R
gene expression value
C
MGUS
SMM
MM
Median mRNA expression (-ΔCt)
IL21R
CCR5
CD40
SLAMF7
MGUS n°6
SMM n°11
MM n°13
D
Mean mRNA expression (-ΔCt)
IL21R
CCR5
CD40
SLAMF7
w/o osteolysis
w osteolysis

Figure 3

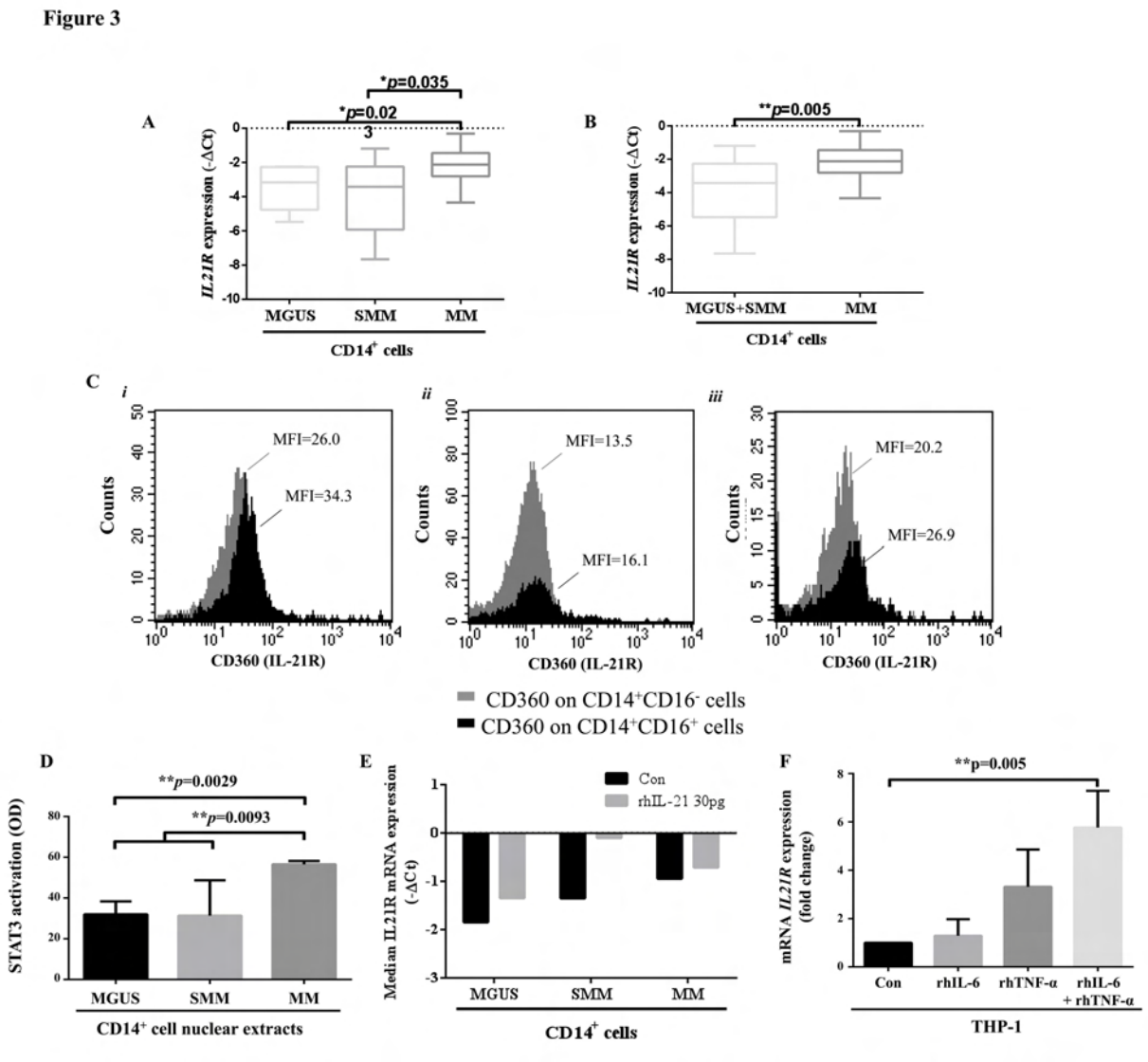
A
*p=0.035
*p=0.02
IL21R expression (-ΔCt)
MGUS
SMM
MM
CD14+ cells
B
**p=0.005
IL21R expression (-ΔCt)
MGUS+SMM
MM
CD14+ cells
C
i
ii
iii
Counts
MFI=26.0
MFI=34.3
MFI=13.5
MFI=16.1
MFI=20.2
MFI=26.9
CD360 (IL-21R)
CD360 on CD14+CD16- cells
CD360 on CD14+CD16+ cells
D
**p=0.0029
**p=0.0093
STAT3 activation (OD)
MGUS
SMM
MM
CD14+ cell nuclear extracts
E
Con
rhIL-21 30pg
Median IL21R mRNA expression (-ΔCt)
MGUS
SMM
MM
CD14+ cells
F
**p=0.005
mRNA IL21R expression (fold change)
Con
rhIL-6
rhTNF-α
rhIL-6 + rhTNF-α
THP-1

Figure 4

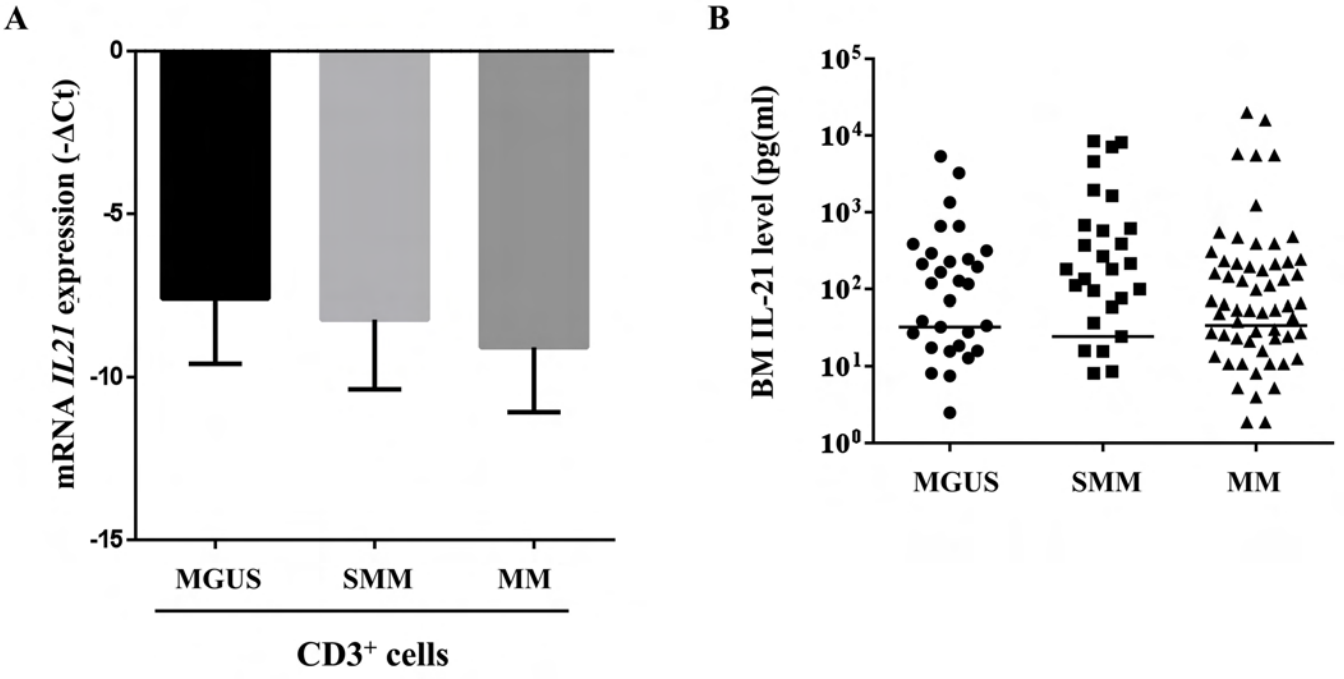
A
0
-5
-10
-15
mRNA IL21 expression (-ΔCt)
MGUS
SMM
MM
CD3+ cells
B
10^5
10^4
10^3
10^2
10^1
10^0
BM IL-21 level (pg(ml)
MGUS
SMM
MM

Figure 5

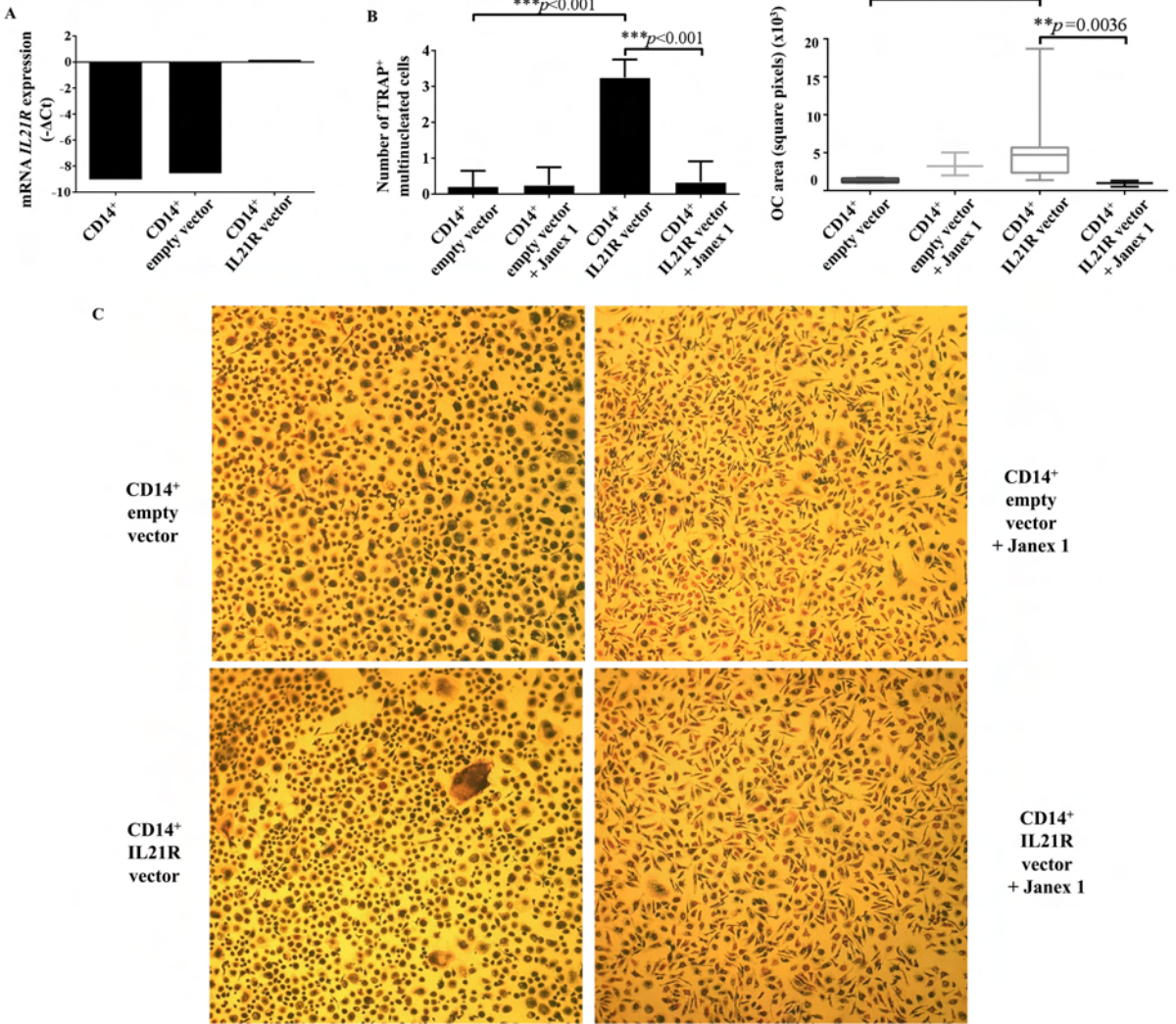
A
mRNA IL21R expression (-ΔCt)
2
0
-2
-4
-6
-8
-10
CD14+
CD14+ empty vector
CD14+ IL21R vector
B
***p<0.001
***p<0.001
Number of TRAP+ multinucleated cells
4
3
2
1
0
CD14+ empty vector
CD14+ empty vector + Janex 1
CD14+ IL21R vector
CD14+ IL21R vector + Janex 1
**p=0.0034
**p=0.0036
OC area (square pixels) (x10³)
20
15
10
5
0
CD14+ empty vector
CD14+ empty vector + Janex 1
CD14+ IL21R vector
CD14+ IL21R vector + Janex 1
C
CD14+ empty vector
CD14+ empty vector + Janex 1
CD14+ IL21R vector
CD14+ IL21R vector + Janex 1

Figure 6

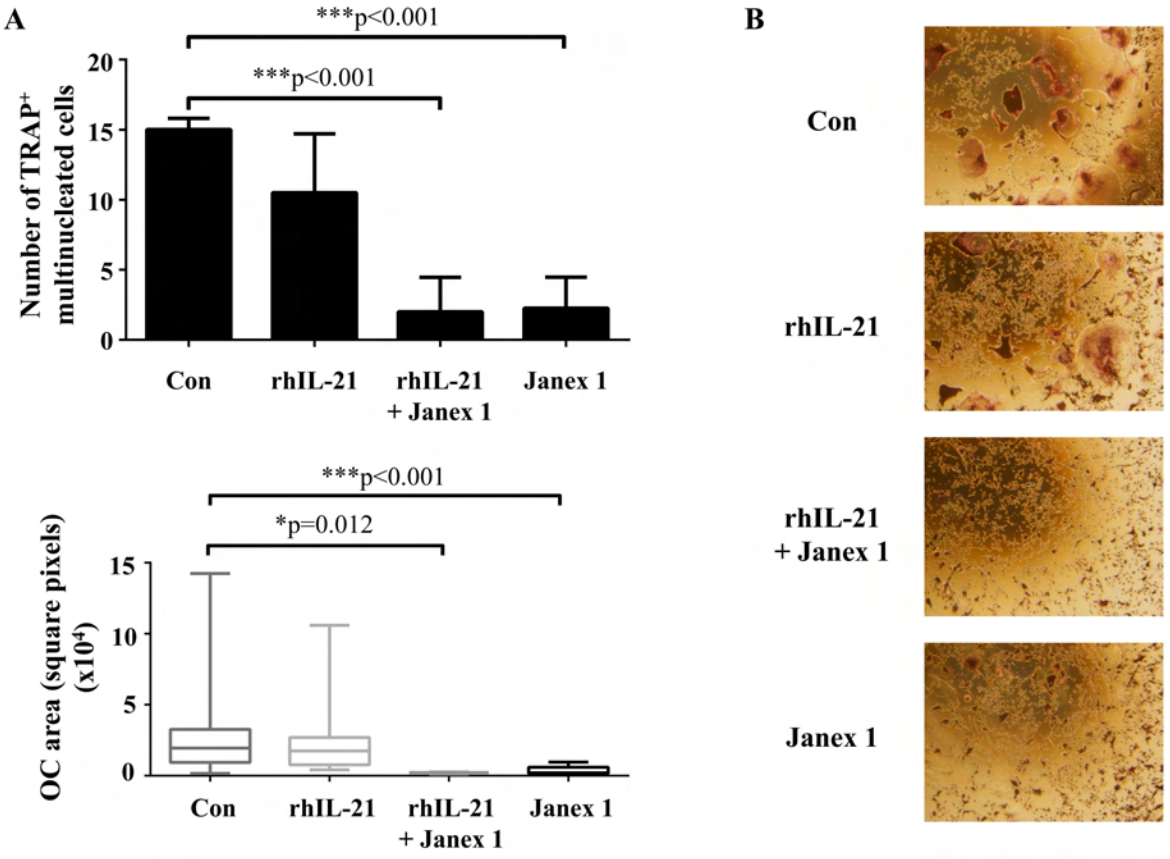
A
***p<0.001
***p<0.001
Number of TRAP+ multinucleated cells
20
15
10
5
0
Con
rhIL-21
rhIL-21 + Janex 1
Janex 1
***p<0.001
*p=0.012
OC area (square pixels) (x10^4)
15
10
5
0
Con
rhIL-21
rhIL-21 + Janex 1
Janex 1
B
Con
rhIL-21
rhIL-21 + Janex 1
Janex 1

SUPPLEMENTAL METHODS

Immunophenotype of BM CD14$^+$ in patients with monoclonal gammopathies.

Briefly, 100 μl of total BM aspirate was incubated in the dark with anti-human HLA-DR-PE (clone L243; BD), anti-human CD14-PerCP-Cy 5.5, anti-human CD16-PE-Cy7 (clone B73.1; BD) and anti-human CD45-APC-H 7 (clone 2D1; BD) for 20 min. Flow cytometry analysis was performed as 6-color experiment by using BD FACS Canto II with Diva software. First, a gate was set around monocytes based on their light-scatter properties. Then, two monocyte populations were defined in that gate: the classical CD14^{bright}CD16$^-$ monocytes and CD14^{dim}CD16^{bright} monocytes. In some experiments, 10^6 mononuclear cells (MNCs), obtained from BM aspirates by density gradient centrifugation (Lympholite-H; Burlington, NC), were stained with anti-human CD14-PerCP-Cy 5.5, anti-human CD16-PE-Cy7 and anti-human CD360/IL-21R APC (Clone 17A12; BD), using the gating strategy described above.

Fluorescence in situ hybridization (FISH) analysis.

FISH analysis has been performed on purified CD138$^+$ cells to test the presence of: hyperdiploidy (ON9RED/15GREEN; Kreatech Diagnostics; Durham, NC); del(13q) (D13 S319SO/CEP 12SG; Metasystems; Altlussheim, Germany); del(17p) (LSI ATM SG/p53SO; Metasystems); chromosome 14 translocation (14 BREAK-APART; Metasystems). If samples were positive for chromosome 14 translocation, the presence of t(4;14) (FGFR3SO/IGHSG; Abbott Laboratories; Abbott Park, IL), t(11;14) (LSI IGH/CCND1XT; Abbott Laboratories) and t(14;16) (IGH/MAF; Abbott Laboratories) were checked.

Microarrays analysis

Total RNA was extracted from BM CD14$^+$ cells using the RNeasy total RNA isolation kit (Qiagen; Hilden, Germany). Gene expression profiles of BM CD14$^+$ cells previously isolated were generated on GeneChip® HG-U133 Plus 2.0 arrays (Affymetrix; Santa Clara, CA). The biotin-labeled cRNA was prepared according to the Affymetrix GeneChip Expression Analysis Technical Manual

protocol. Log2-transformed expression values were extracted from CEL files and normalized using RMA procedure in the *affy* package for Bioconductor and the annotations included in the cdf definition files version 20 available at the Brainarray portal (http://brainarray.mbni.med.umich.edu/Brainarray/Database/CustomCDF/20.0.0/version.html).

Unsupervised and supervised analyses of gene expression data were carried out using the Significant Analysis of Microarrays (SAM) software version 4.00, as previously reported.[13]

Data were deposited in NCBI's Gene Expression Omnibus and are accessible through GEO series accession number GSE70345.

Correlation between *IL21R* expression and that of *CCR5*, *CD40* and *SLAMF7* by BM monocytes arisen from gene expression analysis were evaluated by Spearman *rho* correlation test.

Real Time PCR.

RNA (0,5 µg) was reverse-transcribed with 400 U Moloney murine leukemia reverse transcriptase (Applied Biosystems, Life Technologies) in accordance with the manufacturer's protocol. Real Time PCR was performed by adding complementary DNA to a universal master Mix primers and TaqMan probes (Applied Biosystems) for the following genes: *IL21R*: Hs00222310_m1, *SLAMF7*: Hs00221793_m1 and *ABL*: Hs01104728_m1. The Real Time ready assays for *CCR5* (Assay ID: 104069) and *CD40* (Assay ID: 100254) genes were purchased from Roche Diagnostics (Mannheim, Germany). The expression of selected genes was checked by Real Time PCR by Light Cycler 480 (Roche Diagnostics). To normalize the differences in RNA quality and reverse transcription efficiency, we applied the comparative Ct method using the endogenous reference gene ABL. In the experiments where treated cells were compared to untreated controls, the fold change in mRNA expression (n-fold) of each analyzed gene was calculated as $2^{-\Delta\Delta Ct}$, as previously described.[30] However, when the aim of the analysis was to check the differences between groups of patients, mRNA expression levels were expressed as $-\Delta Ct$.

STAT3 activity assay.

STAT3 activity was evaluated by means of an ELISA-based commercially available kit (Trans AM STAT Family, Active Motif, Vinci Biochem; Vinci, Florence, Italy), used in accordance with the manufacturers' procedures. We tested duplicates of nuclear extracts (each containing 5 μg of proteins) of $CD14^+$ cells purified from 3 MGUS, 3 SMM and 3 MM patients and nuclear extracts of HepG2 treated with rhIL-6 (100 ng/ml) were used as positive controls, as suggested in the manufacturers' procedures. Cell nuclear extracts were obtained and total amount of proteins quantified as previously described.[30]

BM IL-21 levels in patients with monoclonal gammopathies.

The levels of IL-21 in BM plasma were measured in a total cohort of 76 newly diagnosed MM, 42 SMM and 41 MGUS patients. Plasma (5 ml) was obtained after centrifugation from BM aspirates, aliquoted and stored at -20°C until analysis. BM IL-21 plasma levels were detected by Human Interleukin-21 ELISA kit (BioVendor; Brno, Czech Republic), following the manufacturers' protocol.

SUPPLEMENTAL TABLES

Supplemental Table 1: mRNA expression levels of *CD14* (929_at) and *SDC1* (6382_at). Monocyte samples reported in italic style were excluded from gene expression analysis due to high PC contamination according to 2-groups stratification based on K-means clustering of *SDC1* expression.

Monocyte sample	***CD14***	***SDC1***
MGUS1	8789.818	40.304
MGUS2	9006.552	38.80391
MGUS3	6403.874	35.66097
MGUS4	9964.512	43.99736
MGUS5	8146.314	59.22493
MGUS6	8589.581	57.34123
MGUS7	7803.366	44.29881
MGUS8	9120.798	35.85622
MGUS9	8895.179	32.07205
SMM1	8114.306	37.218
SMM2	8029.939	39.68942
SMM3	7796.826	28.66408
SMM4	9010.986	43.27907
SMM5	8058.92	43.83396
SMM6	9088.744	52.35158
SMM7	7662.433	43.14486
SMM8	5344.555	46.07221
SMM9	8406.226	36.69782
SMM10	11324.39	60.34423
SMM11	9027.734	48.58276
SMM12	7547.065	37.88982
SMM13	7526.294	65.80806
SMM14	8964.173	28.70343
SMM15	8211.26	45.07396
MM1	7492.444	32.61221
MM2	6873.478	163.3324
MM3	6079.989	42.57115
MM4	8406.226	70.01866
MM5	6458.982	49.30689
MM6	5512.166	55.35385
MM7	10195.97	37.92994
MM8	8460.027	33.74889
MM9	7921.082	80.19244
MM10	7397.48	47.13206
MM11	11284.27	30.44155
MM12	7538.09	64.00715

MM13	8060.529	100.2527
MM14	9567.787	37.23853
MM15	8702.203	166.6147
MM16	8484.997	99.10607
MM17	8436.607	35.66015
MM18	8612.851	35.29721
MM19	5049.836	56.44912
MM20	8848.109	74.04942
MM21	7571.708	61.97922
MM22	9838.354	104.0483
MM23	9886.636	45.53263
MM24	*4579.45*	*655.08*
MM25	*5069.29*	*1464.04*
MM26	*7199.53*	*1209.62*
MM27	*1372.92*	*7674.54*
MM28	*7325.70*	*702.92*
MM29	*8592.04*	*1117.68*
MM30	*7947.35*	*2153.92*
MM31	*5844.00*	*555.92*
MM32	*5309.73*	*2219.51*

Abbreviations: MGUS, Monoclonal Gammopathy of Undetermined Significance; SMM, Smoldering Multiple Myeloma; MM, Multiple Myeloma.

Supplemental Table 2: List of genes significantly modulated in BM monocytes across the three groups of patients (MM, SMM and MGUS) by multiclass analysis of gene expression data.

Gene ID	Gene Name	SAM Score(d)*
FCER1A	Fc fragment of IgE receptor Ia	1.49
SLCO4C1	solute carrier organic anion transporter family member 4C1	1.46
PTPN22	protein tyrosine phosphatase, non-receptor type 22	1.45
PADI4	peptidyl arginine deiminase 4	1.45
SLAMF7	SLAM family member 7	1.44
PGM1	phosphoglucomutase 1	1.38
RAB37	RAB37, member RAS oncogene family	1.34
RPS17	ribosomal protein S17	1.33
FLVCR2	feline leukemia virus subgroup C cellular receptor family member 2	1.33
ANXA6	annexin A6	1.32
SERPINB10	serpin family B member 10	1.32
WLS	wntless Wnt ligand secretion mediator	1.31
CLTCL1	clathrin heavy chain like 1	1.29
TMEM55A	transmembrane protein 55A	1.26
SSBP4	single stranded DNA binding protein 4	1.25
GNGT2	G protein subunit gamma transducin 2	1.22
LOC100506844	uncharacterized LOC100506844	1.22
CPNE2	copine 2	1.22
CCR5	C-C motif chemokine receptor 5	1.21
UBR4	ubiquitin protein ligase E3 component n-recognin 4	1.21
SQLE	squalene epoxidase	1.20
CTSL	cathepsin L	1.20
SLC9A3R1	SLC9A3 regulator 1	1.20
PNMA1	paraneoplastic Ma antigen 1	1.19
LGALS12	galectin 12	1.19
CHST7	carbohydrate sulfotransferase 7	1.19
LHFPL2	lipoma HMGIC fusion partner-like 2	1.19
MYB	MYB proto-oncogene, transcription factor	1.19
ADA	adenosine deaminase	1.18
SRPK1	SRSF protein kinase 1	1.17
CENPK	centromere protein K	1.17
RUNX3	runt related transcription factor 3	1.17
VAMP5	vesicle associated membrane protein 5	1.16
IL21R	interleukin 21 receptor	1.16
HADHA	hydroxyacyl-CoA dehydrogenase/3-ketoacyl-CoA thiolase/enoyl-CoA hydratase , alpha subunit	1.15
TMEM170B	transmembrane protein 170B	1.14
FBN2	fibrillin 2	1.14
NCAPD2	non-SMC condensin I complex subunit D2	1.14

MTSS1	MTSS1, I-BAR domain containing	1.13
CCL18	C-C motif chemokine ligand 18	1.13
EIF2D	eukaryotic translation initiation factor 2D	1.13
TCN2	transcobalamin 2	1.12
DGKZ	diacylglycerol kinase zeta	1.12
AZU1	azurocidin 1	1.12
SLC2A9	solute carrier family 2 member 9	1.11
CDCA7	cell division cycle associated 7	1.11
TUBB	tubulin beta class I	1.11
SPNS3	sphingolipid transporter 3	1.10
TMEM51	transmembrane protein 51	1.10
KBTBD11	kelch repeat and BTB domain containing 11	1.10
IPCEF1	interaction protein for cytohesin exchange factors 1	1.10
ECRP	ribonuclease A family member 2 pseudogene	1.10
SCCPDH	saccharopine dehydrogenase	1.09
ORM1	orosomucoid 1	1.08
GAS2L1	growth arrest specific 2 like 1	1.08
ANP32E	acidic nuclear phosphoprotein 32 family member E	1.08
ADAMTS5	ADAM metallopeptidase with thrombospondin type 1 motif 5	1.08
GOT2	glutamic-oxaloacetic transaminase 2	1.08
MIR205	microRNA 205	1.07
NECTIN2	nectin cell adhesion molecule 2	1.07
KIF11	kinesin family member 11	1.07
NRM	nurim	1.07
CTSV	cathepsin V	1.07
SIPA1L2	signal induced proliferation associated 1 like 2	1.07
SLC26A8	solute carrier family 26 member 8	1.07
EMB	embigin	1.06
FAM101B	refilin B	1.06
MKI67	marker of proliferation Ki-67	1.06
CDCA7L	cell division cycle associated 7 like	1.06
HEG1	heart development protein with EGF like domains 1	1.06
B4GALT6	beta-1,4-galactosyltransferase 6	1.05
IGF1R	insulin like growth factor 1 receptor	1.05
DNASE2	deoxyribonuclease 2, lysosomal	1.05
IFNGR2	interferon gamma receptor 2	1.05
SELM	selenoprotein M	1.05
EIF3L	eukaryotic translation initiation factor 3 subunit L	1.05
TRAF5	TNF receptor associated factor 5	1.05
TMC8	transmembrane channel like 8	1.05
E2F8	E2F transcription factor 8	1.05
PRRG2	proline rich and Gla domain 2	1.05
CIT	citron rho-interacting serine/threonine kinase	1.04
PTCH1	patched 1	1.04
PSRC1	proline and serine rich coiled-coil 1	1.04
INSIG1	insulin induced gene 1	1.04
MRPL37	mitochondrial ribosomal protein L37	1.04

RRAS	related RAS viral oncogene homolog	1.04
MAP4K4	mitogen-activated protein kinase kinase kinase kinase 4	1.04
PIM1	Pim-1 proto-oncogene, serine/threonine kinase	1.03
IFITM1	interferon induced transmembrane protein 1	1.03
HIP1	huntingtin interacting protein 1	1.03
ANLN	anillin actin binding protein	1.03
PGD	phosphogluconate dehydrogenase	1.03
SPOCK1	SPARC/osteonectin, cwcv and kazal like domains proteoglycan 1	1.03
ISG20	interferon stimulated exonuclease gene 20	1.03
LOC152225	uncharacterized LOC152225	1.03
BPI	bactericidal/permeability-increasing protein	1.03
CKAP4	cytoskeleton associated protein 4	1.03
ZBED3	zinc finger BED-type containing 3	1.02
PKM	pyruvate kinase, muscle	1.02

*Linear discriminant score defined by the Significance Analysis of Microarrays (SAM) analysis.

Supplemental Table 3: List of genes differentially expressed by BM monocytes obtained from supervised analysis of MM patients as compared to SMM.

DOWN

Gene ID	Gene Name	SAM score(d)*	Fold Change
PTPN22	protein tyrosine phosphatase, non-receptor type 22	-4.76	0.59
PADI4	peptidyl arginine deiminase 4	-4.65	0.44
FCER1A	Fc fragment of IgE receptor Ia	-4.62	0.42
SLCO4C1	solute carrier organic anion transporter family member 4C1	-4.57	0.45
RAB37	RAB37, member RAS oncogene family	-4.54	0.58
ECRP	ribonuclease A family member 2 pseudogene	-4.46	0.47
SERPINB10	serpin family B member 10	-4.38	0.29
PGM1	phosphoglucomutase 1	-4.29	0.64
RPS17	ribosomal protein S17	-4.29	0.79
FBN2	fibrillin 2	-4.18	0.54
LGALS12	galectin 12	-4.16	0.60
ANXA6	annexin A6	-4.08	0.65
MIR205	microRNA 205	-4.02	0.76
SPNS3	sphingolipid transporter 3	-3.99	0.64
TMEM55A	transmembrane protein 55A	-3.98	0.67
SCCPDH	saccharopine dehydrogenase	-3.97	0.72
ADAMTS5	ADAM metallopeptidase with thrombospondin type 1 motif 5	-3.97	0.73
SLC2A9	solute carrier family 2 member 9	-3.96	0.74
WLS	wntless Wnt ligand secretion mediator	-3.92	0.64
KBTBD11	kelch repeat and BTB domain containing 11	-3.88	0.66
SRPK1	SRSF protein kinase 1	-3.86	0.69
PGD	phosphogluconate dehydrogenase	-3.85	0.72
SLC26A8	solute carrier family 26 member 8	-3.85	0.66
UBR4	ubiquitin protein ligase E3 component n-recognin 4	-3.82	0.74
LOC100506844	uncharacterized LOC100506844	-3.78	0.62
SLC9A3R1	SLC9A3 regulator 1	-3.78	0.70
CLTCL1	clathrin heavy chain like 1	-3.76	0.70
CENPK	centromere protein K	-3.73	0.43
MYB	MYB proto-oncogene, transcription factor	-3.71	0.51
EMB	embigin	-3.70	0.55
TMC8	transmembrane channel like 8	-3.68	0.74
EIF2D	eukaryotic translation initiation factor 2D	-3.61	0.78
MTMR11	myotubularin related protein 11	-3.60	0.63
BPI	bactericidal/permeability-increasing protein	-3.55	0.42
MRPL33	mitochondrial ribosomal protein L33	-3.53	0.81
NRM	nurim	-3.52	0.79
FMO5	flavin containing monooxygenase 5	-3.52	0.72

HIP1	huntingtin interacting protein 1	-3.52	0.75
KIF21B	kinesin family member 21B	-3.51	0.78
B4GALT6	beta-1,4-galactosyltransferase 6	-3.49	0.77
DGKZ	diacylglycerol kinase zeta	-3.49	0.74
CDA	cytidine deaminase	-3.48	0.65
HDDC2	HD domain containing 2	-3.46	0.78
MARC1	mitochondrial amidoxime reducing component 1	-3.46	0.61
MAP4K4	mitogen-activated protein kinase kinase kinase kinase 4	-3.46	0.79
TMEM170B	transmembrane protein 170B	-3.43	0.62
CPNE2	copine 2	-3.43	0.73
ADGRA2	adhesion G protein-coupled receptor A2	-3.43	0.70
IPCEF1	interaction protein for cytohesin exchange factors 1	-3.42	0.61
CACNA2D3	calcium voltage-gated channel auxiliary subunit alpha2delta 3	-3.41	0.60
MAP4K1	mitogen-activated protein kinase kinase kinase kinase 1	-3.41	0.74
CDCA7	cell division cycle associated 7	-3.41	0.50
PKM	pyruvate kinase, muscle	-3.40	0.69
RNASE2	ribonuclease A family member 2	-3.40	0.58
PSRC1	proline and serine rich coiled-coil 1	-3.40	0.73
CKAP4	cytoskeleton associated protein 4	-3.39	0.65
FAM101B	refilin B	-3.39	0.62
SPOCK1	SPARC/osteonectin, cwcv and kazal like domains proteoglycan 1	-3.38	0.65
NME8	NME/NM23 family member 8	-3.38	0.74
CYTL1	cytokine like 1	-3.37	0.62

UP

Gene ID	**Gene Name**	**SAM score(d)***	**Fold Change**
SLAMF7	SLAM family member 7	4.74	2.44
CCR5	C-C motif chemokine receptor 5	4.55	2.26
CTSL	cathepsin L	4.46	2.13
CHST7	carbohydrate sulfotransferase 7	4.33	1.87
LHFPL2	lipoma HMGIC fusion partner-like 2	4.15	2.20
PNMA1	paraneoplastic Ma antigen 1	4.07	1.55
SSBP4	single stranded DNA binding protein 4	4.06	1.28
PIM1	Pim-1 proto-oncogene, serine/threonine kinase	4.03	1.63
GAS2L1	growth arrest specific 2 like 1	3.98	1.37
GNGT2	G protein subunit gamma transducin 2	3.97	1.40
TCN2	transcobalamin 2	3.91	1.50
FLVCR2	feline leukemia virus subgroup C cellular receptor family member 2	3.90	1.51
YES1	YES proto-oncogene 1, Src family tyrosine kinase	3.87	1.22
SQLE	squalene epoxidase	3.86	1.84
VAMP5	vesicle associated membrane protein 5	3.85	1.62
ADA	adenosine deaminase	3.83	1.79
CTSV	cathepsin V	3.81	1.43

IFNGR2	interferon gamma receptor 2	3.75	1.38

*Ratio of change in gene expression to standard deviation.

Supplemental Table 4: List of differentially expressed genes by BM monocytes arisen from supervised analysis of MM *versus* (MGUS plus SMM) patients.

DOWN

Gene ID	Gene Name	SAM Score(d)*	Fold Change
FCER1A	Fc fragment of IgE receptor Ia	-5.70	0.40
SLCO4C1	solute carrier organic anion transporter family member 4C1	-5.65	0.45
PADI4	peptidyl arginine deiminase 4	-5.58	0.46
PTPN22	protein tyrosine phosphatase, non-receptor type 22	-5.57	0.60
PGM1	phosphoglucomutase 1	-5.35	0.64
RPS17	ribosomal protein S17	-5.15	0.79
ANXA6	annexin A6	-5.12	0.64
RAB37	RAB37, member RAS oncogene family	-5.12	0.60
WLS	wntless Wnt ligand secretion mediator	-5.03	0.63
SERPINB10	serpin family B member 10	-5.01	0.32
CLTCL1	clathrin heavy chain like 1	-4.92	0.68
TMEM55A	transmembrane protein 55A	-4.89	0.67
LOC100506844	uncharacterized LOC100506844	-4.71	0.62
UBR4	ubiquitin protein ligase E3 component n-recognin 4	-4.66	0.74
SLC9A3R1	SLC9A3 regulator 1	-4.63	0.70
CPNE2	copine 2	-4.59	0.71
MYB	MYB proto-oncogene, transcription factor	-4.58	0.51
CENPK	centromere protein K	-4.54	0.43
SRPK1	SRSF protein kinase 1	-4.53	0.70
LGALS12	galectin 12	-4.52	0.63
TMEM170B	transmembrane protein 170B	-4.40	0.61
HADHA	hydroxyacyl-CoA dehydrogenase/3-ketoacyl-CoA thiolase/enoyl-CoA hydratase , alpha subunit	-4.38	0.83
EIF2D	eukaryotic translation initiation factor 2D	-4.37	0.78
DGKZ	diacylglycerol kinase zeta	-4.33	0.74
CDCA7	cell division cycle associated 7	-4.29	0.50
FBN2	fibrillin 2	-4.26	0.58
AZU1	azurocidin 1	-4.25	0.45
IPCEF1	interaction protein for cytohesin exchange factors 1	-4.25	0.61
TUBB	tubulin beta class I	-4.23	0.68
SPNS3	sphingolipid transporter 3	-4.23	0.65
NCAPD2	non-SMC condensin I complex subunit D2	-4.22	0.59
ANP32E	acidic nuclear phosphoprotein 32 family member E	-4.17	0.72
ADAMTS5	ADAM metallopeptidase with thrombospondin type 1 motif 5	-4.17	0.72
ORM1	orosomucoid 1	-4.17	0.49
KIF11	kinesin family member 11	-4.14	0.40
NRM	nurim	-4.14	0.79

KBTBD11	kelch repeat and BTB domain containing 11	-4.13	0.69
GOT2	glutamic-oxaloacetic transaminase 2	-4.13	0.75
SLC2A9	solute carrier family 2 member 9	-4.12	0.76
FAM101B	refilin B	-4.11	0.63
EMB	embigin	-4.10	0.56
CDCA7L	cell division cycle associated 7 like	-4.08	0.54
SLC26A8	solute carrier family 26 member 8	-4.07	0.68
B4GALT6	beta-1,4-galactosyltransferase 6	-4.07	0.77
E2F8	E2F transcription factor 8	-4.05	0.44
MKI67	marker of proliferation Ki-67	-4.04	0.54
EIF3L	eukaryotic translation initiation factor 3 subunit L	-4.04	0.81
PSRC1	proline and serine rich coiled-coil 1	-4.00	0.74
MRPL37	mitochondrial ribosomal protein L37	-3.99	0.84
ANLN	anillin actin binding protein	-3.99	0.44
SPOCK1	SPARC/osteonectin, cwcv and kazal like domains proteoglycan 1	-3.97	0.66
MAP4K4	mitogen-activated protein kinase kinase kinase kinase 4	-3.96	0.80
ZBED3	zinc finger BED-type containing 3	-3.95	0.70
HIP1	huntingtin interacting protein 1	-3.94	0.76
CKAP4	cytoskeleton associated protein 4	-3.93	0.67
CIT	citron rho-interacting serine/threonine kinase	-3.92	0.65
PKM	pyruvate kinase, muscle	-3.92	0.71
RAB27A	RAB27A, member RAS oncogene family	-3.90	0.71
ZWINT	ZW10 interacting kinetochore protein	-3.90	0.49
FOXM1	forkhead box M1	-3.89	0.61
S100A12	S100 calcium binding protein A12	-3.89	0.69
CENPH	centromere protein H	-3.87	0.59
MS4A3	membrane spanning 4-domains A3	-3.87	0.43
PECR	peroxisomal trans-2-enoyl-CoA reductase	-3.86	0.67
TOP2A	topoisomerase II alpha	-3.86	0.40
CDA	cytidine deaminase	-3.84	0.67
CENPF	centromere protein F	-3.83	0.55
LOC100288637	OTU deubiquitinase 7A pseudogene	-3.82	0.59
BPI	bactericidal/permeability-increasing protein	-3.82	0.46
SCCPDH	saccharopine dehydrogenase	-3.82	0.76
GPSM2	G-protein signaling modulator 2	-3.82	0.63
TMC8	transmembrane channel like 8	-3.81	0.77
ZNF281	zinc finger protein 281	-3.81	0.73
MRPL33	mitochondrial ribosomal protein L33	-3.80	0.81
MIR205	microRNA 205	-3.80	0.79
MARC1	mitochondrial amidoxime reducing component 1	-3.79	0.65
HIPK2	homeodomain interacting protein kinase 2	-3.79	0.75
KIF18B	kinesin family member 18B	-3.78	0.50
NCAPG	non-SMC condensin I complex subunit G	-3.78	0.47
RETN	resistin	-3.78	0.58
TPCN1	two pore segment channel 1	-3.77	0.81
TYMS	thymidylate synthetase	-3.77	0.44

RACGAP1	Rac GTPase activating protein 1	-3.77	0.56
SHCBP1	SHC binding and spindle associated 1	-3.77	0.56
GINS1	GINS complex subunit 1	-3.76	0.51
CACNA2D3	calcium voltage-gated channel auxiliary subunit alpha2delta 3	-3.76	0.63
PTDSS1	phosphatidylserine synthase 1	-3.76	0.82
ECRP	ribonuclease A family member 2 pseudogene	-3.75	0.54
PGD	phosphogluconate dehydrogenase	-3.75	0.76
KIAA0101	KIAA0101	-3.74	0.46
MSL1	male specific lethal 1 homolog	-3.74	0.81
TPX2	TPX2, microtubule nucleation factor	-3.73	0.48
TK1	thymidine kinase 1	-3.73	0.66
FAM217B	family with sequence similarity 217 member B	-3.73	0.67
NUSAP1	nucleolar and spindle associated protein 1	-3.73	0.51
NCAPG2	non-SMC condensin II complex subunit G2	-3.72	0.62
KIF20A	kinesin family member 20A	-3.72	0.47
BMX	BMX non-receptor tyrosine kinase	-3.71	0.72
KIF15	kinesin family member 15	-3.70	0.50
HMGB2	high mobility group box 2	-3.69	0.78
IGF1R	insulin like growth factor 1 receptor	-3.69	0.73
NME8	NME/NM23 family member 8	-3.68	0.76
KIFC1	kinesin family member C1	-3.68	0.72
MEGF9	multiple EGF like domains 9	-3.68	0.62
OIP5	Opa interacting protein 5	-3.68	0.54
MAP4K1	mitogen-activated protein kinase kinase kinase kinase 1	-3.67	0.76
ADGRA2	adhesion G protein-coupled receptor A2	-3.67	0.71
CEP55	centrosomal protein 55	-3.67	0.47
TACC3	transforming acidic coiled-coil containing protein 3	-3.65	0.75
NUF2	NUF2, NDC80 kinetochore complex component	-3.64	0.50
RASSF1	Ras association domain family member 1	-3.64	0.82
GPI	glucose-6-phosphate isomerase	-3.64	0.79
CENPM	centromere protein M	-3.63	0.62
ZNF367	zinc finger protein 367	-3.62	0.51
EFCAB2	EF-hand calcium binding domain 2	-3.61	0.67
CTH	cystathionine gamma-lyase	-3.61	0.53
KIF21B	kinesin family member 21B	-3.60	0.80
HIST1H4C	histone cluster 1 H4 family member c	-3.60	0.57
PCNA	proliferating cell nuclear antigen	-3.59	0.62
MTMR11	myotubularin related protein 11	-3.59	0.68
TMC4	transmembrane channel like 4	-3.58	0.72
C20orf27	chromosome 20 open reading frame 27	-3.58	0.78
PLD1	phospholipase D1	-3.58	0.81
UBE2C	ubiquitin conjugating enzyme E2 C	-3.57	0.54
TTK	TTK protein kinase	-3.57	0.50
FAM110B	family with sequence similarity 110 member B	-3.56	0.76
CBX4	chromobox 4	-3.56	0.78
FARSB	phenylalanyl-tRNA synthetase beta subunit	-3.55	0.80

MAD2L1	MAD2 mitotic arrest deficient-like 1	-3.54	0.54
FMO5	flavin containing monooxygenase 5	-3.54	0.76
ERG	ERG, ETS transcription factor	-3.53	0.85
ANAPC15	anaphase promoting complex subunit 15	-3.53	0.82
FAM64A	family with sequence similarity 64 member A	-3.52	0.70
KIF14	kinesin family member 14	-3.51	0.55
SLC25A40	solute carrier family 25 member 40	-3.51	0.75
THBS4	thrombospondin 4	-3.50	0.79
SSR1	signal sequence receptor subunit 1	-3.50	0.85
POLR3B	RNA polymerase III subunit B	-3.50	0.79
PCMT1	protein-L-isoaspartate O-methyltransferase	-3.49	0.78
SIDT1	SID1 transmembrane family member 1	-3.48	0.71
ITGAM	integrin subunit alpha M	-3.47	0.76
CAT	catalase	-3.47	0.72
NCL	nucleolin	-3.46	0.87
LPGAT1	lysophosphatidylglycerol acyltransferase 1	-3.46	0.76
CCNE2	cyclin E2	-3.45	0.62
HAL	histidine ammonia-lyase	-3.45	0.73
MCM7	minichromosome maintenance complex component 7	-3.45	0.72
STMN1	stathmin 1	-3.44	0.79
BIRC5	baculoviral IAP repeat containing 5	-3.44	0.64
SDHD	succinate dehydrogenase complex subunit D	-3.44	0.82
CDC20	cell division cycle 20	-3.43	0.50
PHKA2	phosphorylase kinase regulatory subunit alpha 2	-3.43	0.83
MPO	myeloperoxidase	-3.43	0.49
BUB1B	BUB1 mitotic checkpoint serine/threonine kinase B	-3.43	0.55
DTL	denticleless E3 ubiquitin protein ligase homolog	-3.43	0.51
RRM2	ribonucleotide reductase regulatory subunit M2	-3.43	0.46
TFF3	trefoil factor 3	-3.43	0.80
VRK1	vaccinia related kinase 1	-3.42	0.74
PTTG1	pituitary tumor-transforming 1	-3.42	0.64
TSPAN2	tetraspanin 2	-3.42	0.69
SLC40A1	solute carrier family 40 member 1	-3.42	0.45
GYS1	glycogen synthase 1	-3.42	0.79
KIF4A	kinesin family member 4A	-3.42	0.56
NPIPB15	nuclear pore complex interacting protein family member B15	-3.41	0.73
PLCL2	phospholipase C like 2	-3.41	0.77
TOP1MT	topoisomerase I, mitochondrial	-3.40	0.75
TCF19	transcription factor 19	-3.40	0.67
SFXN5	sideroflexin 5	-3.40	0.87
MELK	maternal embryonic leucine zipper kinase	-3.39	0.56
CYTL1	cytokine like 1	-3.39	0.65
CSF3R	colony stimulating factor 3 receptor	-3.38	0.82
MCM4	minichromosome maintenance complex component 4	-3.36	0.73
USP48	ubiquitin specific peptidase 48	-3.36	0.78
CDK1	cyclin dependent kinase 1	-3.35	0.54

CIDEB	cell death-inducing DFFA-like effector b	-3.35	0.76
CARS2	cysteinyl-tRNA synthetase 2, mitochondrial	-3.35	0.80
IVNS1ABP	influenza virus NS1A binding protein	-3.34	0.74
DLGAP5	DLG associated protein 5	-3.34	0.43
TMEM106C	transmembrane protein 106C	-3.34	0.71
RCC1	regulator of chromosome condensation 1	-3.33	0.85
ASPM	abnormal spindle microtubule assembly	-3.33	0.54
GTSE1	G2 and S-phase expressed 1	-3.32	0.73
BZW2	basic leucine zipper and W2 domains 2	-3.32	0.83
RNASE2	ribonuclease A family member 2	-3.32	0.63
EP300-AS1	EP300 antisense RNA 1	-3.32	0.85
SMC2	structural maintenance of chromosomes 2	-3.31	0.65
RALGAPA2	Ral GTPase activating protein catalytic alpha subunit 2	-3.31	0.84
CCNA2	cyclin A2	-3.31	0.55
VILL	villin like	-3.30	0.83
SSRP1	structure specific recognition protein 1	-3.30	0.82
GGH	gamma-glutamyl hydrolase	-3.30	0.65
SMYD2	SET and MYND domain containing 2	-3.30	0.81

UP

Gene ID	**Gene Name**	**SAM Score(d)***	**Fold Change**
SLAMF7	SLAM family member 7	5.56	2.35
FLVCR2	feline leukemia virus subgroup C cellular receptor family member 2	5.01	1.58
SSBP4	single stranded DNA binding protein 4	4.81	1.29
GNGT2	G protein subunit gamma transducin 2	4.71	1.41
SQLE	squalene epoxidase	4.64	1.81
PNMA1	paraneoplastic Ma antigen 1	4.58	1.52
ADA	adenosine deaminase	4.55	1.75
VAMP5	vesicle associated membrane protein 5	4.49	1.61
IL21R	interleukin 21 receptor	4.48	1.49
RUNX3	runt related transcription factor 3	4.47	1.62
LHFPL2	lipoma HMGIC fusion partner-like 2	4.44	2.03
MTSS1	MTSS1, I-BAR domain containing	4.38	1.43
TCN2	transcobalamin 2	4.25	1.45
CTSL	cathepsin L	4.22	1.87
TMEM51	transmembrane protein 51	4.22	1.71
CHST7	carbohydrate sulfotransferase 7	4.20	1.68
CCR5	C-C motif chemokine receptor 5	4.20	1.95
NECTIN2	nectin cell adhesion molecule 2	4.13	1.25
HEG1	heart development protein with EGF like domains 1	4.08	1.51
SIPA1L2	signal induced proliferation associated 1 like 2	4.07	1.34
TRAF5	TNF receptor associated factor 5	4.05	1.36
DNASE2	deoxyribonuclease 2, lysosomal	4.05	1.60
INSIG1	insulin induced gene 1	4.01	1.69

RRAS	related RAS viral oncogene homolog	4.01	1.48
IFITM1	interferon induced transmembrane protein 1	4.00	2.52
PTCH1	patched 1	3.99	1.12
ISG20	interferon stimulated exonuclease gene 20	3.98	1.68
LOC152225	uncharacterized LOC152225	3.97	1.43
PIM1	Pim-1 proto-oncogene, serine/threonine kinase	3.96	1.58
IFNGR2	interferon gamma receptor 2	3.95	1.34
CD9	CD9 molecule	3.94	2.26
PRRG2	proline rich and Gla domain 2	3.94	1.20
LFNG	LFNG O-fucosylpeptide 3-beta-N-acetylglucosaminyltransferase	3.92	1.37
GAS2L1	growth arrest specific 2 like 1	3.91	1.31
DHRS9	dehydrogenase/reductase 9	3.91	1.77
PAPSS2	3'-phosphoadenosine 5'-phosphosulfate synthase 2	3.91	1.49
CTSV	cathepsin V	3.88	1.36
MAP3K7CL	MAP3K7 C-terminal like	3.87	1.94
EPSTI1	epithelial stromal interaction 1	3.87	2.05
STAT4	signal transducer and activator of transcription 4	3.83	1.40
AMPD1	adenosine monophosphate deaminase 1	3.82	1.72
CASP5	caspase 5	3.79	1.64
MARCO	macrophage receptor with collagenous structure	3.79	1.47
CD40	CD40 molecule	3.78	1.29
SELM	selenoprotein M	3.78	1.55
CACNA1A	calcium voltage-gated channel subunit alpha1 A	3.77	1.25
ZDHHC23	zinc finger DHHC-type containing 23	3.76	1.24
HIVEP2	human immunodeficiency virus type I enhancer binding protein 2	3.75	1.34
LINC00847	long intergenic non-protein coding RNA 847	3.74	1.42
IDI1	isopentenyl-diphosphate delta isomerase 1	3.72	1.27
PRORSD1P	prolyl-tRNA synthetase associated domain containing 1, pseudogene	3.72	1.22
GJA3	gap junction protein alpha 3	3.71	1.16
ADGRE2	adhesion G protein-coupled receptor E2	3.71	1.50
TESK1	testis-specific kinase 1	3.70	1.21
LAP3	leucine aminopeptidase 3	3.69	1.44
MLLT11	myeloid/lymphoid or mixed-lineage leukemia; translocated to, 11	3.68	1.31
SLC16A6	solute carrier family 16 member 6	3.67	1.50
EIF5A2	eukaryotic translation initiation factor 5A2	3.66	1.29
PIK3IP1	phosphoinositide-3-kinase interacting protein 1	3.64	1.21
IFI27	interferon alpha inducible protein 27	3.62	3.13
ERGIC1	endoplasmic reticulum-golgi intermediate compartment 1	3.60	1.25
CXCL11	C-X-C motif chemokine ligand 11	3.60	2.01

*Ratio of change in gene expression to standard deviation.

Supplemental Table 5: IL-21 expression by BM microenvironment cells.

	-ΔCt
BM MSCs	ND
$CD14^+$ cells	ND
$CD138^+$ cells	ND
$CD3^+$ cells	-8,3
Activated $CD3^+$ cells	-1
$CD8^+$ cells	ND
$CD4^+$ cells	-8,6

Abbreviation: ND=not detectable

LEGENDS OF SUPPLEMENTAL FIGURES

Supplemental Figure 1: BM monocytes purity. Representative flow cytometry plots to assess the purity of BM monocytes after purification with anti-CD14 Ab conjugated microbeads. Monocytes were identified as $CD14^+CD45^+CD138^-$ cells.

Supplemental Figure 2: Monocyte sub-population sorting. Example of flow cytometry analysis with anti-human CD16 and anti-human CD14, showing the two sub-population of monocytes before **(A)** and after **(B, C)** sorting. Purity of $CD14^+CD16^+$ **(B)** and $CD14^+CD16^-$ **(C)** cells.

Supplemental Figure 3: Gene expression profiling of purified BM $CD14^+$ cells from patients with different monoclonal gammopathies. (A) Heatmap of the differentially expressed genes resulted from the multiclass Significant Analysis of Microarrays (SAM) of the monocytes samples clustered according to the diagnosis of the patients. Heatmaps of the differentially expressed genes arisen from the supervised SAM analyses comparing BM $CD14^+$ cells from MM *versus* SMM **(B)** or active MM *versus* asymptomatic forms (MGUS plus SMM) **(C)**.

SUPPLEMENTAL FIGURES

Supplemental Figure 1

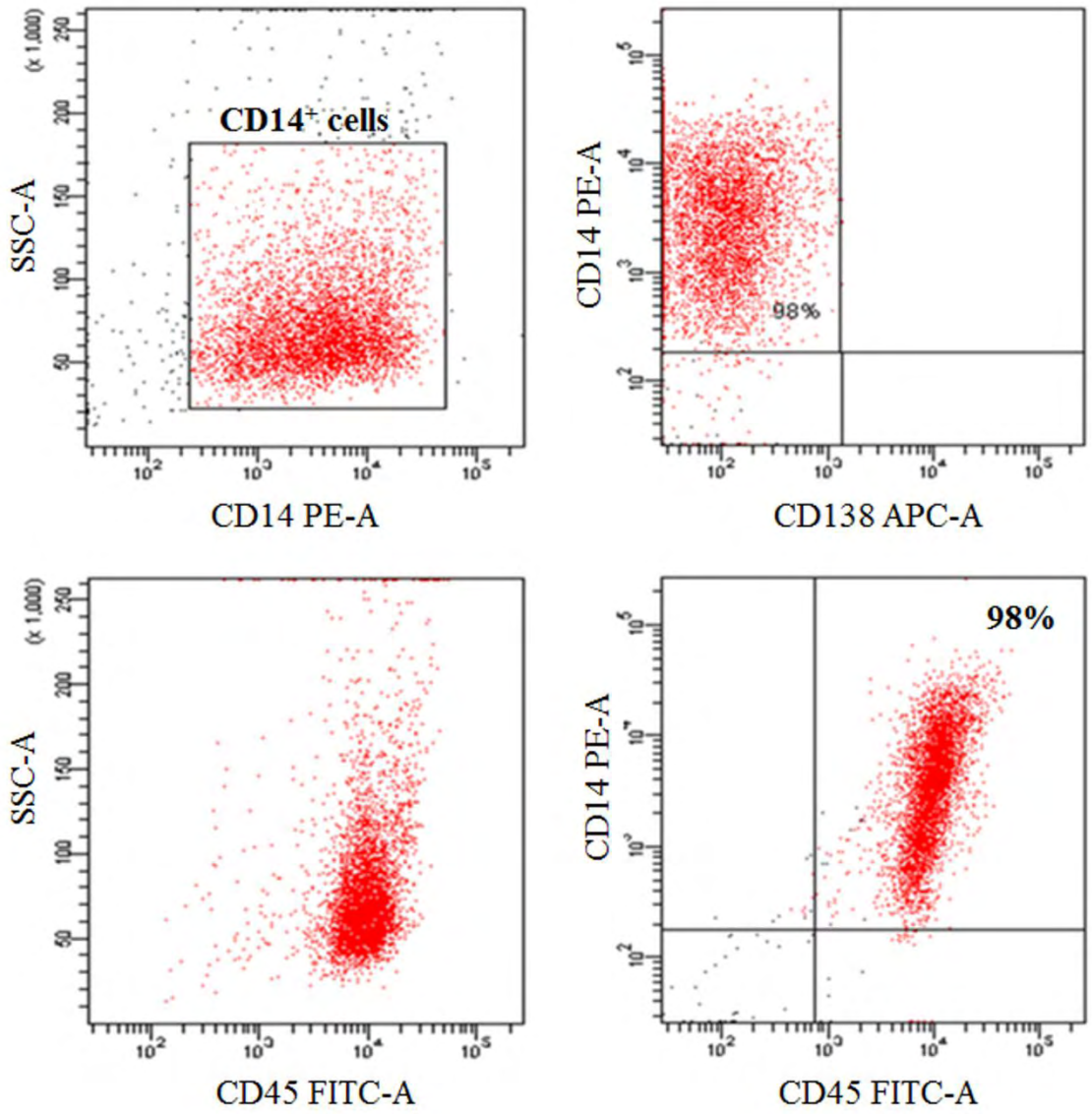

Supplemental Figure 2

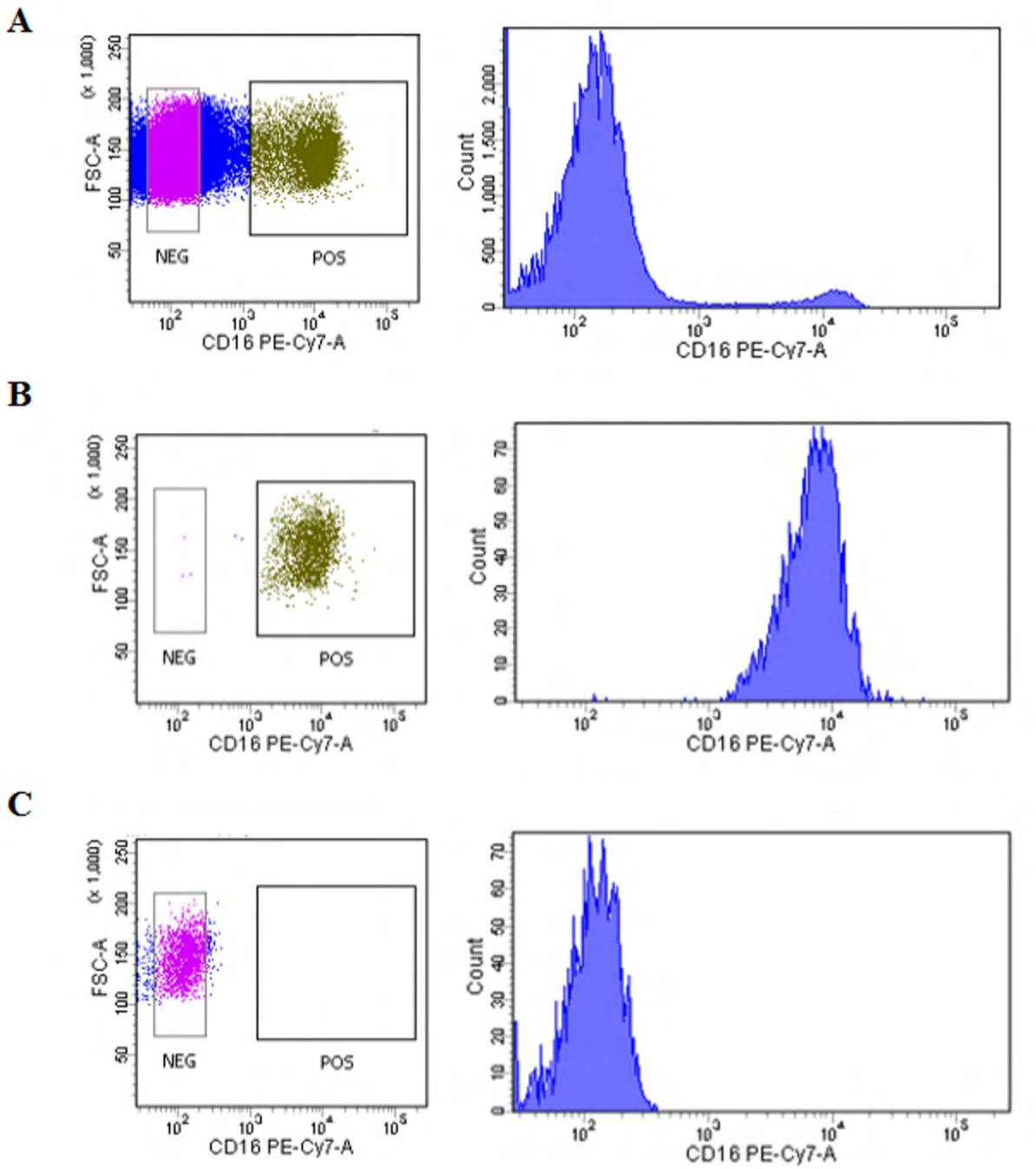

Supplemental Figure 3